6 Track Issues

Tore Dahlberg

CONTENTS

I. THE RAILWAY TRACK AS A DYNAMIC SYSTEM

The purpose of a railway track is to guide the trains in a safe and economic manner. The track and the switches should allow smooth passage of the trains. If the track is not perfectly levelled and aligned, the irregularities will cause oscillations or vibrations of the train, and this may induce discomfort for passengers and damage for goods. Long wavelength undulations of the track will give rise to low-frequency oscillations of the train and short wavelength irregularities cause vibrations and noise, both in the train and in the environment. Oscillations, vibrations, and noise may become unpleasant for the train passengers and for people in the vicinity of the railway line.

This chapter focuses on different aspects of track dynamics and train–track interaction. Dynamic properties of the track as a whole and the different components of the track will be investigated. In the first part of this chapter the dynamics of the complete track structure will be discussed including the dynamics of the compound train–track system, followed by how dynamic properties of some track components are treated.

A. The Track and Its Components

A railway track structure consists of rails, sleepers, railpads, fastenings, ballast, subballast, and subgrade, see Figure 6.1. Sometimes, for example, in tunnels, the ballast bed is omitted and the rails are fastened to concrete slabs resting on the track foundation. Two subsystems of a ballasted track structure can be distinguished: the superstructure, composed of rails, sleepers, ballast, and subballast, and the substructure (subgrade, subground) composed of a formation layer and the ground. First, a short description of the different parts of the ballasted track and their functions will be given. Then, the function of the complete track structure will be discussed.

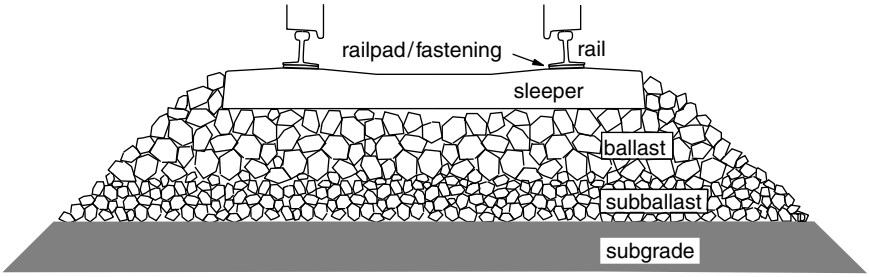

FIGURE 6.1 Track with its different components: rails, railpads, and fastenings (fastenings not shown in this figure, see Figure 6.2), sleepers, ballast, subballast, and subgrade (subground).

B. Rails

A modern steel rail has a flat bottom and its cross section is derived from an I-profile. The upper flanges of the I-profile have been converted to form the railhead. The English engineer Charles Vignoles has been credited the invention of this design in the 1830s. In Europe, one commonly used rail profile is the UIC60 rail (with a Vignoles profile), where 60 refers to the mass of the rail in kg per meter.

The rails should provide smooth running surfaces for the train wheels and they should guide the wheelsets in the direction of the track. The rails also carry the vertical load of the train and distribute the load over the sleepers. Lateral forces from the wheelsets, and longitudinal forces due to traction and braking of the train should also be transmitted to the sleepers and further down into the track bed. The rails also act as electrical conductors for the signalling system.

C. Railpads

In a railway track with concrete sleepers, railpads are placed between the steel rails and the sleepers, see Figure 6.2. The railpads protect the sleepers from wear and impact damage, and they provide electrical insulation of the rails. Wooden sleepered tracks may not have rail pads.

From a track dynamics point of view, the railpads play an important role. They influence the overall track stiffness. When the track is loaded by the train, a soft railpad permits a larger deflection of the rails and the axle load from the train is distributed over more sleepers. Also, soft railpads isolate high-frequency vibrations. They suppress the transmission of high-frequency vibrations down to the sleepers and further down into the ballast. A stiff railpad, on the other hand,

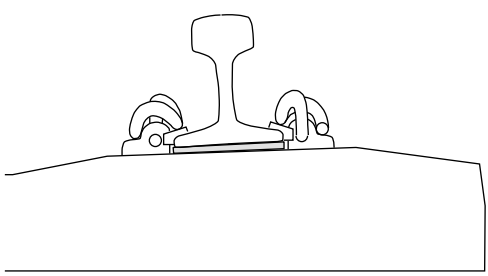

FIGURE 6.2 Rail fastened to sleeper with railpad inserted between the rail and the sleeper. Rail is fastened to the sleeper by fastening clips, with an electrical insulation between the rail and the clip.

gives a more direct transmission of the axle load, including the high-frequency load variations, down to the sleepers below the wheels.

D. Sleepers (or Crossties)

The sleepers provide support of the rails and preserve gauge, level, and alignment of the track. The sleepers transmit vertical, lateral, and longitudinal forces from the rail down to the ballast bed. They should also provide electrical insulation between the two rails.

Nowadays, ballasted railway tracks are usually constructed with monobloc concrete sleepers (for example, twin-bloc concrete sleepers are used in France). Timber sleepers have been used almost since the beginning of railway construction. In countries where the timber price is acceptable, timber sleepers are still frequently used. Sometimes, it is suitable to use steel sleepers.

E. Ballast

Coarse stones are used to form the bed (a ballast bed) of the railway track. The sleepers to which the rails are fastened are embedded in the ballast. The ballast layer supports the track (the rails and the sleepers) against vertical and lateral forces from the trains. It is tightly compacted or tamped around the sleepers to keep the track precisely levelled and aligned. The standard depth of ballast is 0.3 m, but it is packed to 0.5 m around the sleeper ends to ensure lateral stability. Traditionally, angular, crushed, uniformly graded hard stones and rocks (granite, limestone, slag, or other crushed stone) have been considered good ballast materials. However, availability and economic motives have often been prime factors considered in the selection of ballast materials. From a physical point of view, the ballast materials and their interactions are complex. Constitutive laws of ballast materials are under development.

F. Subballast

Subballast is material chosen as a transition layer between the upper layer of large-particle, good quality ballast and the lower layer of fine-graded subgrade. The subballast used in most new constructions is intended to prevent the mutual penetration of the subgrade and the ballast and to reduce frost penetration. Any sand or gravel materials may serve as subballast material as long as they meet necessary filtering requirements.

G. Geotextiles

Sometimes, geotextiles are used to prevent the intermixing of the subgrade and the subballast. Geotextiles are permeable geomembranes of synthetic fibers. They are used to separate two consecutive layers of granular materials and/or to reinforce a soil layer of insufficient mechanical strength. They can also be used as filters or drainage.

H. Subgrade

Subgrade, or formation, is a surface of earth or rock levelled off to receive a foundation for the track bed. Sometimes, an extra layer, a formation layer, is put on the earth so as to give the correct profile of the track bed. The subballast and ballast layers rest on this material. The subgrade is a very important component in the track structure and has been the cause of track failure and poor track quality, Li and Selig.[1] Unfortunately, in existing tracks the subgrade is not involved in the maintenance operations, and once the track has been laid, little can be done to alter its characteristics, Chrismer and Read.[2]

II. FUNCTION OF THE TRACK

The track should guide the train. It should bring the train safely along the track and through switches to the destination. It should also carry the load of the train and distribute the load over an area that is as large as possible.

A. To Guide the Train

The main function of the track is to guide the train. The two wheels of a wheelset are rigidly connected to the wheel axle. The wheel treads are conical in order to steer the wheelset. If the wheelset is not exactly on the centreline of the track, one wheel will have a larger rolling radius than the other. Due to the rigid connection of the two wheels (via the axle), the wheelset turns towards the centre of the track, and, having passed the centreline, the second wheel will have the larger rolling radius forcing the wheelset back towards the centre. This leads to a sinusoidal movement of the wheelset along the track. It also promotes better radial adjustment of the wheelset in curves. If the lateral movement of the wheelset becomes too large, the flanges of the wheels will prevent derailment. This movement will induce a low-frequency lateral movement of the railway vehicle and lateral forces on the track.

B. To Carry the Load

Another function of the track is to carry the load of the train and to distribute the load over an area of the subgrade that is as large as possible. In a conventional railway track the rails distribute the wheel–rail contact forces over several sleepers. The sleepers, supported by the ballast, transmit the load via the sleeper base area to the ballast, and the ballast disperses the load over a larger area of the subballast and the subgrade. A wheel–rail contact force of, say, 10 t, that is applied over a few square centimetres at the wheel–rail contact patch, is distributed over an area of the subgrade that is, probably, more than one square metre.

III. DYNAMIC PROPERTIES OF THE TRACK

In this section, the dynamics of the entire track structure will be investigated. In Section IV the dynamics of some components of the track will be examined in more detail.

One way to investigate the dynamic properties of a railway track is to load the track with a sinusoidal force. At frequencies up to approximately 200 Hz, this can be carried out by using hydraulic cylinders. If one wants to investigate the track response at higher frequencies, the track may be excited by an impact load, for example, from a sledgehammer. Figure 6.3 shows a typical

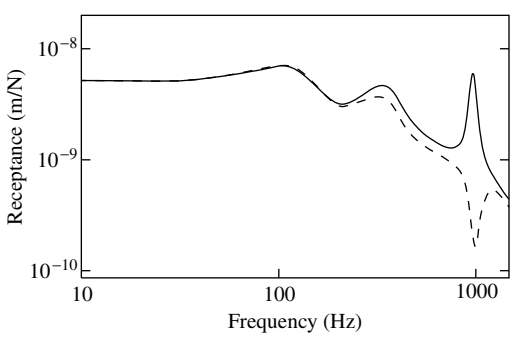

FIGURE 6.3 Typical track receptances when rail is loaded with a sinusoidally varying force. Track receptance when rail is loaded between two sleepers (full-line curve) and above one sleeper (dashed curve) versus loading frequency. The maxima indicate resonance frequencies in the track structure.

receptance curve of a track. The receptance is the ratio of the track deflection and the force put on the track, thus giving deflection in metres per Newton of the load. The receptance is the inverse of the track stiffness, cf. Figure 6.6, where the track stiffness variation along a track is shown. As can be seen in Figure 6.3, the receptance, and thus also the track stiffness, will depend on the frequency of the load. Normally, the receptance also depends on the preload on the track (preload is a static load superimposed to the dynamic load), because most tracks have a nonlinear relationship between load and deflection. (In Figure 6.3 the scale on the ordinate is given just to indicate an overall dynamic range. The curves give the principal behaviour only; these curves differ from one track to another.)

Several well-damped resonances can be found in a track structure. Sometimes, when the track is built on a soft ground, one resonance may appear in the frequency range 20 to 40 Hz, Oscarsson[3] (this resonance is not shown in the figure). This is a resonance when the track, and a great deal of the track substructure, vibrates on, for example, a layered structure of the ground. The track structure itself thus plays a minor role for this resonance. These vibrations can be perceived several metres away from the track. To bring this resonance into a track model, Oscarsson needed to introduce inertia terms from the subground into the dynamic model, see Section III.G.4.

One track resonance is usually obtained in the frequency range 50 to 300 Hz. This resonance is obtained when the track structure (rails and sleepers) vibrates on the ballast bed. The rails and the sleepers provide the "mass" and the ballast provides the "spring" for this resonance vibration. The ballast also provides a large amount of damping, so this resonance is very well damped, see the first, very flat maximum in Figure 6.3 at a frequency slightly above 100 Hz.

Another resonance can often be found in the frequency range 200 to 600 Hz. This resonance is explained by the rail bouncing on the railpads. The railpad acts as a spring inserted between two masses: the rail and the sleeper. Here, the ballast provides most of the damping.

The highest resonance frequency discussed here is the so-called pinned–pinned resonance frequency. This is the resonance that can be seen at approximately 1000 Hz in Figure 6.3. The resonance peak is narrow, indicating that the resonance at this frequency is very lightly damped. The pinned–pinned frequency occurs when the wavelength of the bending waves of the rail is twice the sleeper spacing. In this case, the bending vibration of the rail has nodes at the supports, i.e., at the sleepers. This explains why the pinned–pinned frequency is so lightly damped; mainly the material damping of the steel itself (the rail material) is involved in damping this vibration and very little vibration energy is transmitted to the surroundings (and then mainly as propagating waves along the rail and almost nothing to the ballast).

In Figure 6.3 it can be seen that the track behaves quite differently if the receptance is measured between two sleepers (the full-line curve) or above a sleeper (the dashed curve). When loading the track halfway between two sleepers, and when the track is excited at the pinned–pinned frequency, the pinned–pinned resonance is easily excited. There will be a large deflection of the rail at a unit amplitude force excitation. This gives a peak at 800 to 1000 Hz in the receptance curve (the peak shown by the full-line curve in Figure 6.3 at approximately 1000 Hz). On the other hand, if the rail is excited above a sleeper, i.e., at a node of the pinned–pinned vibration, then the track will be very stiff at this point. Evidently, the track has an anti-resonance at this point (and this frequency). At this excitation, the track deflection must be symmetric with respect to a vertical line through the point of loading. This implies that the slope of the rail is zero at the loaded sleeper. On either side of the load, the rail vibrates with what is approximately the pinned–pinned vibration mode (only very close to the loading point, where the slope is zero, the vibration mode differs from the pinned–pinned mode). This rail vibration then acts as a dynamic vibration absorber making it difficult for the load to excite that point of the track. (Thus, if the pinned–pinned vibration mode had not been there, neither the peak nor the dip would have appeared in the receptance curves at the pinned–pinned frequency.)

If the Euler–Bernoulli beam theory is used, the pinned–pinned frequency can easily be estimated. The frequency f (Hz) (or angular frequency ω in radians per second) is the same as the

fundamental frequency of a simply supported beam of length L, and it is:

$$f = \frac{\omega}{2\pi} = \frac{1}{2\pi}\pi^2\sqrt{\frac{EI}{mL^4}} \tag{6.1}$$

where EI is the bending stiffness of the rail, m is the mass of the rail per unit length, and L is the sleeper spacing. For a UIC60 rail one has, approximately, $m = 60$ kg/m and $EI = 6.4$ MNm^2. If sleeper spacing L is $L = 0.65$ m, one obtains $f = 1214$ Hz. This is, as said, an estimation of the pinned–pinned frequency. In practice, this resonance frequency will be lower than the one calculated here.

The reason why the real pinned–pinned frequency is lower than the frequency given by the formula above is that the Euler–Bernoulli beam theory is not very accurate when the wavelength λ of the vibration is short. The Euler–Bernoulli theory is accurate only when the wavelength of the vibration is much longer than the height of the beam, and here this condition is not fulfilled. The height h of the rail cross section of a UIC60 rail is $h = 172$ mm, and this is not much shorter than the wavelength λ of the pinned–pinned frequency (here $\lambda = 2L = 1.3$ m $= 7.5$ h). In practice, shear deformation of the rail and rotatory inertia should also be included to give a better estimation of the pinned–pinned frequency. This is done in the Rayleigh–Timoshenko beam theory. Using this theory, a lower resonance frequency is obtained (this is discussed further in Section IV.A below). The Rayleigh–Timoshenko beam theory gives, for a UIC60 rail and in this frequency range, a frequency that is 20 to 25% lower than the frequency given by the Euler–Bernoulli theory.

Higher resonance frequencies also occur in the track structure, see Section IV below. These frequencies are of importance for the noise emission of the track, and they are treated in the chapter dealing with noise in this handbook.

A. Nonlinear Track

The discussion above concerns linear tracks, i.e., the relationship between the track displacement and the force loading the track is linear. In practice, however, many tracks are nonlinear, giving a nonlinear relationship between the load on the track and the track deflection. Figure 6.4 shows measurements performed by Banverket (the Swedish National Rail Administration) on a newly built track in Sweden. The rail has been loaded with a sinusoidal force and the part of the force that was transmitted to the sleeper below the load was measured (this part is little more than 50%). Then, the load on the sleeper was plotted as a function of sleeper displacement. The measurements were repeated three times at three adjacent sleepers giving the three curves in Figure 6.4. It is

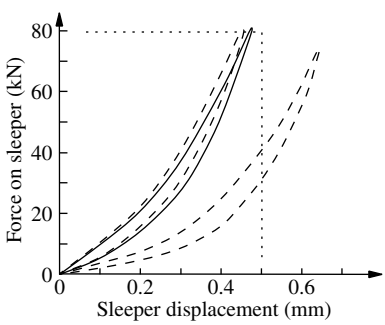

FIGURE 6.4 Measured sleeper displacement when track is loaded with a sinusoidal force (measurements performed by Banverket).

clearly seen in the figure that the relationship between the load on a sleeper and the sleeper displacement is nonlinear, and it is also seen that the ballast stiffness is different below the different sleepers. An extreme case of nonlinearity is when a sleeper is hanging in the rail with a gap between the sleeper and the ballast. One of the sleepers in Figure 6.4 could be such a sleeper that is not fully supported by the ballast.

The nonlinearity implies that the receptance of a track (Figure 6.3) looks different at different load levels. If the track is loaded by a static force (a static preload), and superimposed to that of a dynamic (sinusoidal) force, then the receptance of the track will depend on the preload; a large preload makes the track stiffer, i.e., the curve in Figure 6.3 moves downwards, and many resonance frequencies shift to a higher frequency.

B. Train Moving on Track–Excitation Sources of Train and Track Vibrations

The vibrations and the frequencies discussed so far refer to the track alone. In the case of a train loading the track, the springs and masses of the train (wheelsets, suspensions, bogie frames, and so on) contribute to the dynamic behaviour of the compound train–track system and other resonance frequencies will appear. One such resonance is when the wheelset vibrates as a mass using the track stiffness as the "spring." This resonance may fall in the frequency range 30 to 100 Hz.

One "spring" in the train–track system is obtained at the wheel–rail contact. The elastic deformation at the contact patch can be seen as deformation of a spring with nonlinear characteristics. The stiffness of the "contact spring" increases with increasing wheel–rail contact force. This spring will influence the high-frequency behaviour of the wheel–rail system. (The spring is called a Hertzian spring, named after Hertz who investigated the contact between elastic bodies.)

When the train moves along the track, especially at high speed, other dynamic phenomena appear. Heavier and faster trains induce ground vibrations that are transmitted to buildings along the railway lines. This brings discomfort to people due to noise and vibrations generated in the buildings, Jonsson.[4]

Also, when train speed increases, the intensity of railway-generated noise and vibration generally becomes higher. If the track support is soft, for example, when the track is built on a layer of clay, then the train speed may exceed the velocity of the Rayleigh surface wave in the ground. This will induce a tremendous increase of the vibration level, and train speed must be limited (this happened on the Swedish West Cost Line, where the track had to be removed and the subground strengthened before the trains were allowed to pass at high speed). This topic has been thoroughly investigated by, for example, Krylov.[5]

A large number of excitation sources exist that may induce oscillations, vibrations, and noise in the train and in the track and its surroundings. For the track, four different (and independent) geometric errors, or irregularities, may develop. These errors can be in track alignment, track level, track gauge, and the cant of the track (cant is the superelevation of the outer rail in relation to the inner rail of the track in curves). Long wavelength geometric irregularities in the track alignment will induce lateral displacements of the railway cars, and this will induce travelling discomfort for the passengers. Short wavelength irregularities will induce vibrations and noise. The same can be said for long and short wavelength irregularities of the track level (vertical profile). Irregularities in the track gauge will also induce lateral displacements of the railway cars. Deficiencies or excesses in the cant will induce lateral forces in curves.

Several sources contribute to make the track geometry deteriorate. Track settlement will induce long wavelength irregularities of the track both vertically and laterally. A rail may not be absolutely straight when it comes from the manufacturer and the railhead top surface may not be absolutely plane. Also, when in use, short wavelength periodic irregularities (also called corrugations) may develop on the railhead due to the train traffic. The corrugation generates high-frequency vibration of the rail and the wheel, and noise is emitted.

One source generating train and track vibrations is wheel out-of-roundness. A wheel is seldom perfectly round because when it is used, periodic irregularities may develop on the wheel tread. These irregularities may be of either long wavelengths (so-called polygonalisation with one to five wavelengths around the wheel) or of short wavelength. Especially, short wavelength irregularities often appear on block-braked wheels.

Another source of vibration excitation is the irregular track stiffness. For example, it has already been mentioned that a track is stiffer at a sleeper and more flexible between two sleepers. Thus, there will be a larger deflection of the rail when the wheel is between two sleepers than when it is above one. This induces an excitation of the train and the track at the "sleeper passage frequency." This frequency depends on the sleeper distance and the train speed, and it may, of course, induce resonance vibrations in the train and in the track.

C. Excitation Frequencies

A wheel running with speed v (m/s) over a sinusoidal rail irregularity of wavelength λ (m) will perceive an excitation frequency f (in hertz, Hz) that is:

$$f = \frac{v}{\lambda} \tag{6.2}$$

With vehicle speeds $v = 5$ to 60 m/s and with irregularity wavelengths $\lambda = 0.030$ to 0.300 m one obtains excitation frequencies in the frequency interval $f = 17$ to 2000 Hz. Longer wavelengths give lower frequencies. The excitation will then induce vibrations and noise in the train and in the track structure and the environment. Resonances in the train–track system will also amplify these vibrations at the resonance frequencies.

Three different sources generating train and track vibrations will now be discussed in some detail. These are railhead corrugation (short wavelength irregularities) in Section III.D, long wavelength irregularities in Section III.E and impact loads in Section III.F.

D. Railhead Corrugation (Short Wavelength Periodic Irregularities)

Periodic irregularities of various wavelengths sometimes develop on the railhead and on the wheel tread. Railhead irregularities seem to appear on almost every kind of railway track, from heavy haul tracks to lightweight metropolitan lines. The development of irregularities on the railhead is explained by the dynamics of the train–track system and linked to resonance effects in the combined rail–wheelset system. It is assumed to be so, because the irregularities that develop are periodic of a certain wavelength; mostly in the range 30 to 300 mm. Such periodic irregularities are named corrugation. When the train speed increases, the dynamic interaction between the vehicle and the track becomes more and more pronounced and this gives rise to larger dynamic forces between the wheels and the rails. Once the rail corrugation has begun to develop, the dynamic forces in the train–track system will be further magnified, and the deterioration rate of the track will increase.

Following the wavelength of the periodic irregularities, these are classified in different ways. Here, the irregularities of very short wavelengths are called corrugation; then come short wavelength irregularities and long wavelength irregularities. Unfortunately, different authors use different classifications, and sometimes the word corrugation is used for all wavelengths. In this section, the word corrugation is used for short wavelength railhead periodic irregularities of lengths 300 mm or less. A recent review of studies on rail corrugation was presented by Sato et al.,[6] where a short historical survey on rail corrugation is also given.

1. Classification of Railhead Irregularities

Alias[7] gives an overview of different types of wave formations on the railheads. The irregularities are divided into three categories: corrugation, with wavelength 30 to 80 mm and with amplitudes of a few hundredths of a mm; short waves, with wavelength 150 to 300 mm and with amplitudes up to 1 mm; and long waves, with wavelength up to 2 m. Only the longer wavelengths can be explained by the manufacturing process. Lévy[8] classifies the lengths of the waves as: short waves, 0 to 250 mm; medium waves, 150 to 600 mm; and long waves, 0.3 to 2 m. Lévy also presents a system to measure and analyse undulatory rail wear. Grassie and Kalousek[9] classify the corrugation by mechanisms. Two mechanisms are identified in their paper. First the wavelength-fixing mechanism, i.e., a mechanism that establishes a certain wavelength of the corrugation, and secondly, the damage mechanism, which is a mechanism that generates the unevenness (wear, plastic deformation, etc.). Six classes of corrugation are identified and the authors name the different types of corrugation after where they appear: heavy haul, light rail, booted sleeper, contact fatigue, rutting, and roaring rails. The authors claim that the wavelength fixing mechanism is known in all but one class; the roaring rails. Treatments to avoid or reduce the problem are proposed, Kalousek and Grassie.[10]

Alias[7] refers to the UIC (l'Union Internationale des Chemins de Fer, International Union of Railways) catalogue of rail defects. Two definitions of corrugation are given. One says that "corrugation is characterised by an almost regular sequence of shiny peaks and dark troughs generally spaced approximately 30 to 80 mm apart". For another type of corrugation it is stated that "in this wave effect there is no difference in appearance between the peaks and troughs of the waves", and "the wavelength generally varies between about 80 and 300 mm". Of the latter, the longer waves (300 mm) occur preferentially on the low rails in curves. Thus, railhead irregularities are divided into two groups here: corrugation (30 to 80 mm) and short wavelength irregularities (80 to 300 mm). This corrugation thus develops on the railhead due to the train traffic.

2. Consequences of Rail Corrugation

Clark et al.[11] developed a mathematical model to describe the dynamics of the vehicle-track system. They also performed experiments with two specially prepared test rails; this involved grinding simulated corrugations 60 mm long over a 6 m length of the rails. Their findings were that the rail vibrates out of phase with the corrugations so that the cyclic irregularity seen by the wheel is minimised. This means that all the motion is being induced into the track because the inertia of the rail is so much less than that of the wheel. At certain speeds, sleeper resonances will be excited by the corrugation wavelength. Likely effects of sleeper resonances are ballast degradation and track settlement with loss of vertical track profile. Also, railpads and fastenings (clips) may deteriorate due to the many alternating load cycles, and sleepers may be exposed to fatigue damage due to the cyclic stresses set up in the sleepers in the resonance situation.

3. Origin of Rail Corrugation

The origin of corrugations on rails has not yet been fully explained. Resonance effects between rail, wheel, and axle are believed to be involved. Also, resonance vibration of the portion of the rail between the front and rear wheel of a bogie has been found to be involved in the corrugation growth process, Igeland.[12] Only the long waves (order of metres) can be explained by the rail manufacturing process.

Several hypotheses have been suggested to explain the development of rail corrugation. So far, however, no generally accepted explanation has been given. Probably, different phenomena are involved in creating corrugation of different wavelengths. What makes the corrugation phenomenon especially remarkable is that there does not seem to be any direct relationship between the train

speed and the corrugation wavelength. One idea put forward by some authors is that the short-term dynamic behaviour of the train–track system causes long-term wear to develop. Other authors have tried to refine dynamic models of wheels and track wishing to find a corrugation-initiating mechanism in terms of the short-term behaviour of the wheel–track system. Thus, many authors have tried many different hypotheses to explain the origin of rail corrugation. Some hypotheses will now be presented. (Note that this section is intended as a presentation of different hypotheses put forward to explain the rail corrugation phenomenon. The references given are samples only; for a complete review, please refer to the paper by Sato et al.[6])

Clark and Foster[13] put forward the theory that self-excited vibration characteristics of a flexible wheelset and track system under high creepage conditions may provide possible explanations for the formation of corrugations on the running surface of the rails.

Alias[7] gives some characteristics of wave formation in rails. Some rails have a succession of polished shiny areas which contrast with a duller base on their running surfaces. The shiny patches are 30 to 80 mm apart and are generally quite regularly spaced. The shiny, raised parts correspond to the highest points of the bumps; the dark parts, i.e., the troughs, are oxidised. Metallographic analyses reveal that the peaks have a hardened martensitic structure to a very slight depth (from a few hundredths of a millimetre to 0.2 to 0.3 mm). This structure is explained by slippage of the wheels. The slippage brings about a sharp increase in temperature of the rail surface followed by rapid cooling due to thermal conduction to the surrounding material. As martensite occupies a greater volume than a structure in equilibrium, this is assumed to explain the formation of the peaks. This explanation of the formation of the peaks can be compared with the explanation of the formation of the troughs given by other authors, see for example Igeland.[14] The formation of the troughs is explained by slippage and wear. The wheel–rail friction force and the irregular normal force create the troughs by periodic slippage and wear.

Werner[15] pointed out that the corrugation wavelengths are predominantly integer fractions of the wheel width, and thus can be related to standing surface shear waves in the wheel tread surface.

In a paper by Frederick,[16] it was shown how measured relationships to quantify the dynamic response of the wheel and rail to vertical, lateral, and longitudinal forces can be combined with formulae for the rate of rail wear and wheel–rail creepage to predict whether or not a small wave in the surface of the rail will be deepened or erased by passing axles.

In an approach by Brockley and Ko,[17] it was proposed that corrugations are formed by wear resulting from torsional vibration of the drive wheels and by longitudinal vibration of the rail.

Valdivia,[18] Knothe and Valdivia,[19] and Knothe and Ripke,[20] suggested that corrugation formation can be explained as a feedback process between (a) the wheel and rail high frequency oscillations and (b) long-term wear phenomena. This work has been continued in, for example, Hempelmann and Knothe[21] and in Müller.[22] Müller also introduced a "contact mechanical filter" effect indicating that the wheel–rail contact itself could promote corrugation.

Suda and Iguchi[23] stated that the corrugation growth conditions depend on the natural frequencies of the system. By appropriate selection of the natural frequencies, it would be possible to reduce the development of corrugation of one wavelength without inducing growth of corrugation of other wavelengths. They also stated that the rolling direction and the speed have a great influence on the corrugation growth. Scaled and full-scale roller test stands have been used, Sato et al.[6]

Kalousek[24] suggested that corrugations develop from tiny surface cracks in the rail and that rail life can be substantially increased by preventive grinding.

A linear model giving wear rate as a function of frequency was suggested by Tassilly and Vincent.[25,26] A transfer function between the initial wheel and rail roughness and the wear rate spectrum in the contact patch was presented. Under some conditions, the initial roughness on the rail was shown to degenerate into corrugation in some frequency bands. The model has been used as a tool to design track modifications to prevent the growth of corrugations.

Ideas including plastic deformation of the railhead are put forward by Cervoni and Vincent,[27] Bogacz et al.,[28] and Suda and Iguchi.[23] Böhmer and Klimpel[29] used mathematical models to study the influence of work hardening and residual stresses on corrugation.

Igeland[12] based the corrugation calculation on a semiempirical contact mechanics relationship between creep, friction force, and normal force. The vertical contact forces between the moving wheels and the rails were calculated in the time domain, allowing for a nonlinear Hertzian wheel–rail contact stiffness. It was found that the two wheelsets of a travelling bogie interact via the rail between the wheels, and that both the front and rear wheel of the bogie should be considered in the corrugation growth analysis. In Nielsen[30] a validation of an integrated mathematical model to field observations was made and the agreement between simulations and field observations was good.

E. Long Wavelength Irregularities

Long wavelength irregularities are defined here as irregularities of wavelengths of 300 mm or longer. These irregularities may be either geometric irregularities in the track or on the wheel, or irregularities of the track stiffness.

1. Sleeper Spacing

Even though the rail itself may not have an irregularity with a wavelength corresponding to the sleeper spacing, the wheel will be influenced by the varying stiffness of the track. As the track is stiffer at the sleepers, and softer in-between, the wheel will be excited with a frequency that corresponds to the speed v of the train and the sleeper spacing λ. The excitation frequency f becomes $f = v/\lambda$.

2. Wheel Out-of-Roundness

An out-of-round wheel will excite the train–track structure with one or several frequencies corresponding to the wavelengths of the wheel out-of-roundness. An eccentric wheel will induce the frequency corresponding to the number of wheel revolutions per second (a wheel of radius $r = 0.45$ m gives an irregularity of wavelength $\lambda = 2.8$ m). An oval wheel will induce twice that frequency (wavelength $\lambda/2$), and so on. Also, nonperiodic irregularities may appear on the wheel tread. Especially if the wheel is equipped with block brakes, short wavelength corrugation may develop. A survey is given in Nielsen and Johansson.[31] In Johansson and Nielsen,[32] the influence of different types of out-of-roundness on the vertical dynamic wheel–rail contact force and track response is investigated through extensive field tests and numerical simulations.

3. Rail Manufacturing

The rail manufacturing process may induce rail irregularities. The wavelength of this irregularity is of the order of one to several metres. These irregularities will induce a low-frequency excitation of the train and the track.

4. Track Stiffness Irregularities

Track stiffness variation due to the sleeper spacing has already been mentioned. Other places along the track having variable stiffness are at switches and turnouts. At switches, the sleepers have different lengths and different spacings, and this influences the track stiffness. The symmetry of the track is lost at switches, implying that the left and right rail will have different stiffnesses (the stock rail keeps the stiffness of the track, whereas the switch rail becomes stiffer because of the longer sleepers supporting that rail, see Figure 6.5).

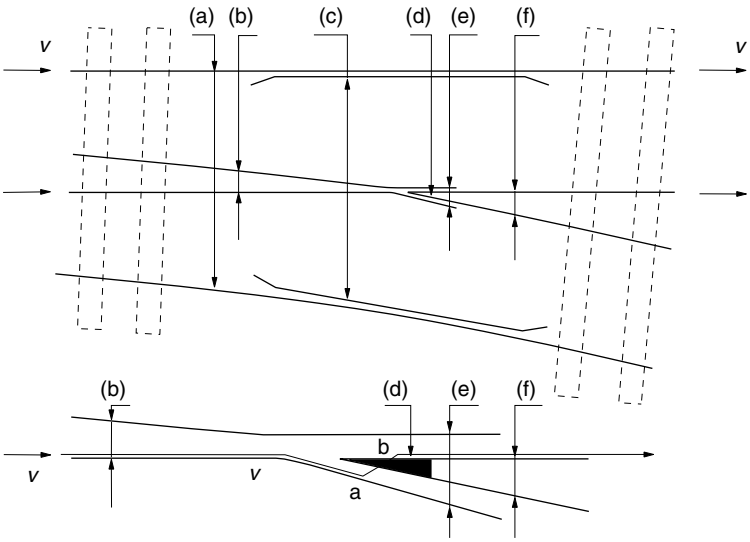

FIGURE 6.5 Railway turnout: (a) stock rails, (b) switch rails, (c) guard rails, (d) nose, (e) wing rails, and (f) nose rails. Some sleepers are indicated by dashed lines. The entrance and the exit of a wheelset passing straight through the turnout are indicated by arrows. The wheel path through the crossing is shown in the lower, close-up figure. The wheel leaves the wing rail at point a and enters the nose at point b.

Especially if a switch is equipped with a manganese crossing (frog), the rail bending stiffness (*EI*) will change dramatically at the crossing. Such a sudden change of the stiffness will induce transient and high-frequency vibrations in the train and in the track. The mass is also larger at the crossing making inertia forces larger, see Andersson and Dahlberg.[33]

The track superstructure is seldom built on a homogeneous substructure. Due to a variable stiffness of the track subgrade, the track stiffness experienced by the train will vary along the track. As this stiffness is more or less random along the track, it will induce low-frequency random oscillations of the train.

Nowadays, it is possible to measure the vertical track stiffness continuously along the track. Banverket, the Swedish National Rail Administration, has developed a trolley by which the track can be loaded and track stiffness measured while moving along the track at a speed of up to 30 km/h, (see Figure 6.6). A new track stiffness measurement car, by which measurements can be performed at speeds of 70 km/h, has been developed, Berggren.[34] Measured track stiffness along a distance of 3000 m is shown in Figure 6.6. It is seen in the figure that there may be rather rapid changes of the track stiffness, and it is also seen that the track subground has a large influence on the track stiffness. It is seen in the figure (km 11.4 to 11.65) that a pile deck and a bridge make the track very stiff, whereas the light-weight fill makes it very flexible (at km 11.4). A transition area from an embankment to a bridge is also a place where large and rapid changes of the track stiffness may occur.

5. Track Embankment Settlements

When a track is loaded by the weight of the train and, superimposed on that, high-frequency load variations, the ballast and subground may undergo nonelastic deformations. After the load has passed, the track will not return exactly to its original position but to a position very close to the original one. After thousands and thousands of train passages, all these small nonelastic deformations will add, differently in different parts of the track, to give a new track position.

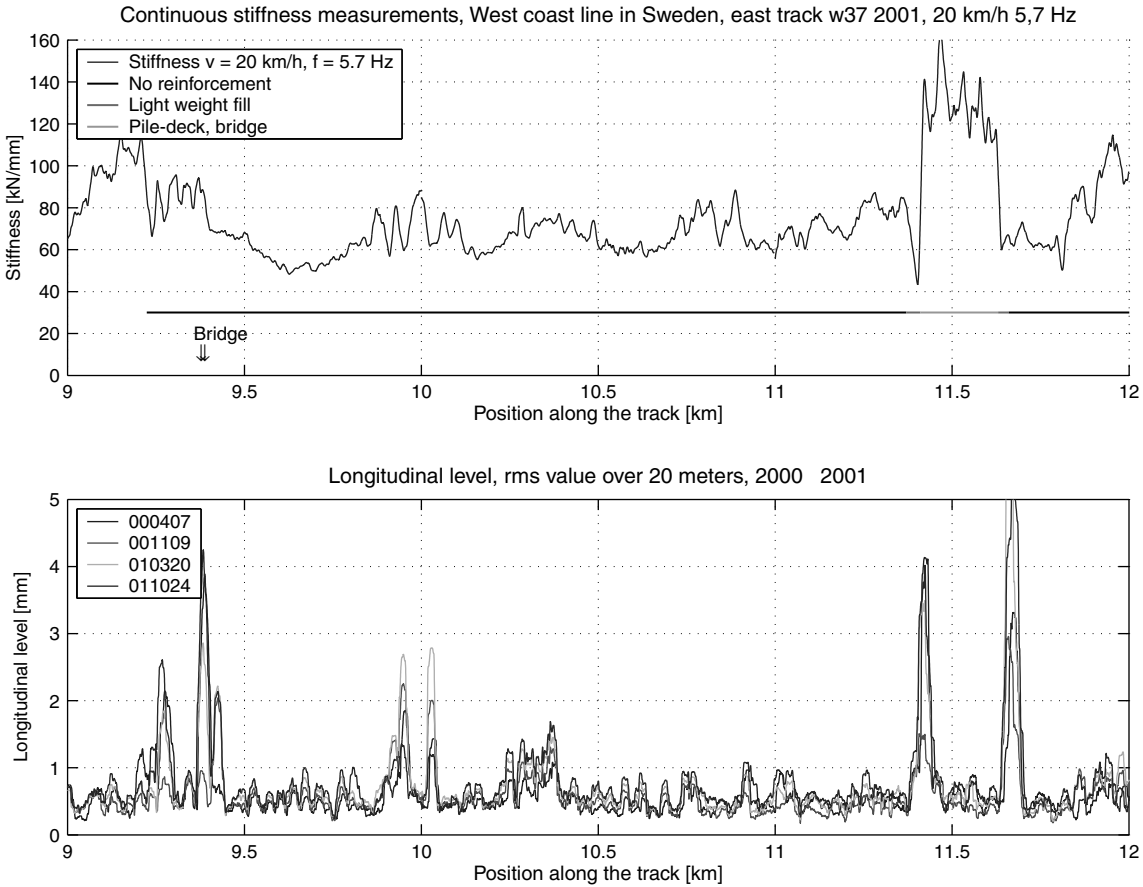

FIGURE 6.6 Track stiffness (axle load divided by track deflection) along railway track as measured by the Banverket track stiffness measurement trolley, and four measurements (during two years) of the longitudinal level of the track (positive downwards, meaning that a large peak in the curve indicates a local settlement of the track). Figure provided by Eric Berggren at Banverket.

This phenomenon is called differential track settlement. The track alignment and the track level will change with time. Depending on the subground, the wavelength of these track irregularities will be of the order of metres up to hundreds of metres. The uneven track will induce low-frequency oscillations of the train. Gradually, the track load variations will increase and so will the track settlement. Especially, the transition area from an embankment to a bridge is a place where track settlements tend to occur, see Figure 6.6. In the lower figure (of Figure 6.6) it can be seen that large track settlements occur at 9.4 km due to a bridge and at 11.4 and 11.7 km due to an embankment and light-weight fill.

F. Impact Loads

In the above two sections (Section III.D and Section III.E), short wavelength irregularities on the railhead and long wave-length irregularities of the track have been discussed. In this section, distinct single impact loadings of the track will be discussed. Such loadings could come from, for example, wheel flats or other defects on the wheel tread, rail joints, and switch crossing (frog) passages.

1. Wheel Flats

It sometimes happens that due to problems with the brakes at a wheel (or due to low adhesion), a wheel does not start to rotate immediately as the train starts or the wheel stops rotating before the train comes to a standstill. Instead, the wheel slides along the rail for a while. When the wheel slides, part of the wheel tread is removed and a flat surface is formed. Later, when the wheel starts to rotate, an impact load will hit the rail at every revolution of the wheel. This load will induce high-frequency vibrations of the track and noise will be emitted. Sometimes the impact load may be so high that the rail is cut off (this may occur at low temperatures). Wheel flat impacts have been investigated by, among others, Fermér and Nielsen.[35]

2. Measurements with Wheelset Having Wheel Flats

Measurements with an instrumented wheelset prepared with wheel flats have been performed by the Swedish National Rail Administration (Banverket). Some of these measurements were reported in Fermér and Nielsen.[35] The wheelset had standard wheels with solid wheel discs. Strain gauges on the wheel discs were used to measure the wheel–rail contact force. After a first test series without wheel flats, artificial wheel flats of 40 mm length were ground on the two wheel treads. To maintain symmetry, the wheel flats were ground with the same position on the left and the right wheel.

In Figure 6.7, measured (figure to the left) and calculated (figure to the right) contact forces between the wheel and the rail are shown. The calculations were performed using the computer program DIFF, developed for calculation of the dynamic interaction between the train and the track, Nielsen[36] (see also Section III.H below). The results shown in Figure 6.7 are for train speed $v = 70$ km/h and for axle load 22 t. It is seen that this relatively small wheel flat induces a large impact load on the rail even if the train speed is not very high.

In Figure 6.8, the bending stress in a sleeper due to the load impact from the wheel flat is shown (measured and calculated, respectively). The wheel flat hits the rail above the sleeper in this case. It is concluded from the figures that the wheel flat causes large dynamic contributions to the contact force and to the stresses in the sleeper.

3. Rail Joints

In the case of welded rail joints, there may be a small difference in level of the two rails connected at the joint. When a wheel, especially at high speed, "climbs" this difference in level, large dynamic forces will arise (or more correctly: as the wheel mass is larger than the rail mass, the wheel will

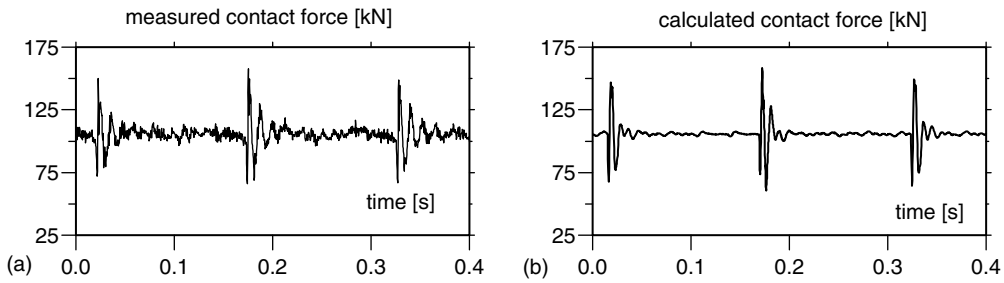

FIGURE 6.7 (a) Measured contact force between wheel and rail when wheel has a wheel flat (left figure), and (b) calculated contact force between wheel and rail (right figure) (Source: From Fermér, M., and Nielsen, J.C.O., *Vehicle Syst. Dyn.*, 23, pp. 142–157, August 23–27, 1993).

"press down" the rail, but this will, of course, also create large dynamic forces). In the case of fishplated joints, or other expansion joints, not only the problem of difference in level appears, but also an irregularity of stiffness will occur at the joint.

4. Switches

When a train passes a switch, dynamic effects will appear due to several factors. As mentioned above, sleepers have another spacing and a different length at the switch, giving a change of track stiffness. When a wheel passes the switch blade and the crossing (the frog, see Figure 6.5), the wheel–rail contact patch will suddenly move laterally on the wheel tread. This implies that the wheel will move laterally to find its new equilibrium position, inducing a longitudinal force on the wheel and on the track and thus a yaw moment on the wheelset. At the crossing, where the wheel moves over from the wing rail to the nose rail (or vice versa) the geometry of the crossing and the wheel profile seldom fit exactly to give a smooth transition. Instead, due to different heights of the wing rail and the nose, this transition often induces a vertical impact load on the wheel and on the crossing, Andersson and Dahlberg.[33]

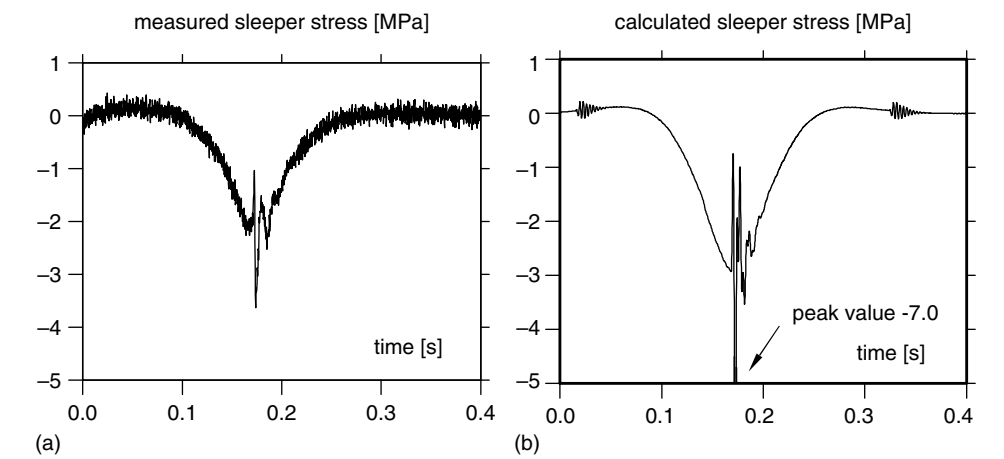

FIGURE 6.8 (a) Measured bending stress in sleeper when load from the wheelflat hits the rail above sleeper (left figure), and (b) calculated bending stress in sleeper (right figure) (Source: From Fermér M., and Nielsen, J.C.O., *Vehicle Syst. Dyn.*, 23, pp. 142–157, August 23–27, 1993).

Another source that induces dynamic effects in switches is the sudden change of rail bending stiffness at the crossing. Especially for cast manganese crossings, two rails meet in one large block containing both the wing rails and the nose rail. At the transition from the rail to the manganese crossing, the stiffness changes dramatically because the manganese block is very stiff. The block is also extremely heavy and the large mass of the crossing contributes to make the wheel–rail impact force at the crossing even worse.

G. Mathematical Modelling of Track Dynamics

In this section, mathematical models used to simulate the train–track dynamic interaction will be presented. The survey mainly focuses on models describing the track deflection in the vertical plane. The following topics will be discussed:

- beam (rail) on continuous elastic foundation (Section III.G.1)
- vehicle-bridge interaction (moving mass on simply supported beam) (Section III.G.2)
- beam (rail) on discrete supports (Section III.G.3)
- beam (rail) on discrete supports including ballast model (Section III.G.4), and
- beams (rails) on sleepers embedded in continuum, including three-dimensional FEM models (Section III.G.5).

1. Beam (Rail) on Continuous Elastic Foundation (Winkler Beam)

The railway track structure consists of the rails, sleepers, railpads, fastenings, ballast, and subgrade. Depending on what one wants to investigate, these components may be modelled in a simpler or a more sophisticated manner. The rail may be modelled either as an ordinary Euler–Bernoulli beam (the conventional beam theory is used) or as a Rayleigh–Timoshenko beam (see Section IV.A). The Rayleigh–Timoshenko beam theory includes the rotatory inertia of the beam cross section and beam deformations due to the shear force. Also, a longitudinal (axial) force in the rail may be included in these models.

In the most simple track model, a beam (that is a model of the rail) rests on a continuous elastic foundation. The foundation is modelled by an evenly distributed linear spring stiffness. The distributed force supporting the beam is then proportional to the beam deflection. This model was introduced by Winkler in 1867 and is still in use for easy and quick track deflection calculations. The only track parameters needed for this model are the beam bending stiffness EI (Nm^2) and the foundation stiffness (the bed modulus) k (N/m^2, i.e., N/m per meter of rail). The rail deflection $w(x)$ (x is the length coordinate) is then obtained from the differential equation:

$$EI\frac{\mathrm{d}^4 w}{\mathrm{d}x^4} + kw(x) = q(x) \tag{6.3}$$

where $q(x)$ is the distributed load on the rail.

This model may be acceptable only for static loading of a track on a soft support, for example, a track with wooden sleepers. No dynamic effects can be analysed using this model as it contains no mass. Especially, the pinned–pinned frequency at approximately 800 to 1000 Hz, when the rail vibrates with nodes at the sleepers, is not contained in this model. On the other hand, using this model it can be seen that the track is lifted in front of the wheel and behind the wheel, see the dashed line in Figure 6.9. This model assumes, however, that there is a tensile force between the rail and the foundation where the track is lifted. In practice, it is only the dead load of the rail and sleepers that will close the "gap" between the track structure and the bed.

To introduce models of railpads, sleepers, and ballast into the track model, the beam may be placed on a bed consisting of several continuous layers instead of the single layer shown in Figure 6.9. The discrete rail supports (railpads and sleepers) are then "smeared out" along the rail

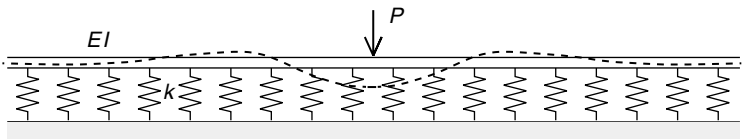

FIGURE 6.9 Beam (bending stiffness *EI*) on elastic foundation (bed modulus *k*). The beam is loaded with a point force *P* from the wheel. The dashed line indicates beam (rail) deflection due to the wheel load *P*.

to give several distributed layers. Nor can this model reproduce the pinned–pinned frequency. A continuous model like this one was used by Grassie and Cox.[37] They examined the behaviour of the track support and it was concluded that large sleeper strains were associated with poorly damped sleeper resonances. Comparisons with British Rail experiments were made. Effects of changes in the support (the railpads) were studied, and it was found that a softer railpad isolates the sleeper more effectively and it will significantly reduce the sleeper strains.

2. Vehicle–Bridge Interaction (Moving Mass on Simply Supported Beam)

So far in this chapter, only the railway track has been considered a dynamic system. A railway bridge is also a dynamic system that interacts with a train passing the bridge. The dynamic interaction of a wheel (a rigid mass) and a simple bridge model (a simply supported beam) will now be investigated.

The well known "moving mass" problem will be discussed. This problem was reviewed and reinvestigated by Månsson.[38] The dynamic interaction between a rigid mass M moving with a constant speed v along a simply supported beam (length L, mass per unit length m, bending stiffness EI) was examined. The system parameters $M/mL = 0.5$ (mass ratio) and vehicle speed $v/v_{\text{ref}} = 0.5$ were used. The reference speed v_{ref} is $v_{\text{ref}} = 2L/T_{\text{e}}$, where the eigenperiod T_{e} of the fundamental (cyclic) eigenfrequency f_{e} of the beam is $T_{\text{e}} = 1/f_{\text{e}} = 2\pi/\omega_{\text{e}}$ and ω_{e} is the fundamental angular eigenfrequency: $\omega_{\text{e}} = \pi^2(EI/mL^4)^{1/2}$. Results obtained by Månsson were then compared with results found in the literature.

The wheel–rail contact force (or, if the simply supported beam is a model of a bridge, the wheel–bridge contact force), as calculated by Månsson with the commercial software LS-DYNA, is shown in Figure 6.10 together with results from two other investigations. The fourth curve in

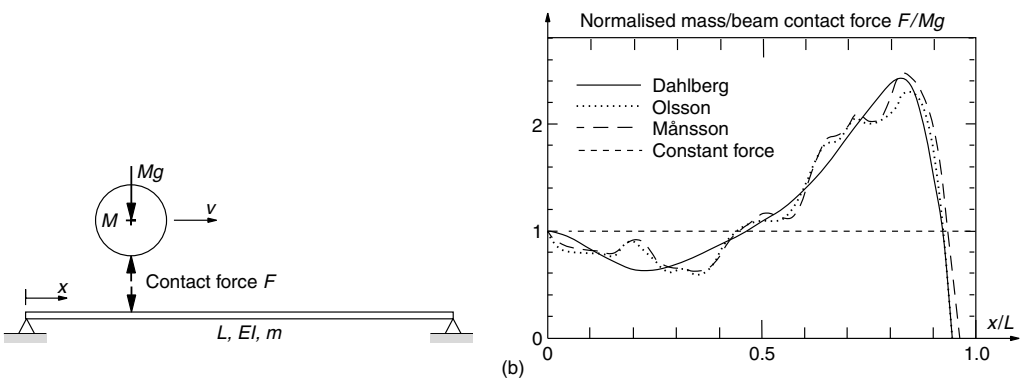

FIGURE 6.10 Contact force between a moving mass M and a simply supported beam. The contact force is calculated by three different methods. The force is normalised with respect to the static load (the weight Mg) of the moving mass. Here mass ratio is $M/mL = 0.5$ and vehicle speed $v/v_{\text{ref}} = 0.5$, where $v_{\text{ref}} = 2L/T_{\text{e}}$ and T_{e} is the eigenperiod of the fundamental frequency of the beam, i.e., $T_{\text{e}} = 2\pi/[\pi^2(EI/mL^4)^{1/2}]$.

Figure 6.10, the straight line, gives the constant force Mg, which is the dead load of the mass. If no dynamic effects were present, then the wheel–bridge force would have been Mg.

The full-line curve in Figure 6.10 was obtained by Dahlberg.[39] Modal analysis (three modes) was used to calculate the beam deflection and it was assumed that the contact force could be written in the form of a polynomial. Due to the low number of modes included, and due to the restriction that the contact force should be written in the form of a polynomial, no high-frequency variations of the contact force could be modelled by that method.

The dotted curve in Figure 6.10, from Olsson,[40] was obtained by use of the finite element method and modal analysis for the beam. Five modes were included in that analysis, which, again, means that high-frequency variations cannot be modelled very accurately (thus, variations with a frequency higher than the fifth eigenfrequency of the beam cannot be modelled with a high accuracy).

The dashed curve, from Månsson,[38] gives the contact force obtained by using the finite element method and a direct time-stepping algorithm for the moving mass problem (no modal analysis is involved). It is noted that the two finite element methods give very similar results apart from a minor deviation around $x/L = 0.80$ to 0.87. One explanation of this discrepancy could be that the modal analysis used in the two first cases (Dahlberg and Olsson) will smooth the variations of the curve and thereby make the maximum at $x/L = 0.82$ slightly too small.

In Figure 6.10, it is seen that the overall behaviour of the wheel–bridge contact force $F = F(x)$ is that initially, when the wheel enters the bridge, the contact force equals the static load of the wheel, i.e., $F(0) = Mg$, but immediately when the wheel starts to load the bridge, the contact force decreases. This happens when the bridge (the beam) starts to deflect under the horizontally moving mass (the wheel). Because of the decrease of the contact force $F(x)$, the dead load Mg of the mass becomes larger than the reaction force $F(x)$ and also the mass will start to move downwards (it follows the deflected beam). After a while the beam deflection will change direction and the beam moves upwards, also pushing the mass upwards. This induces a large contact force between the mass and the beam, and $F(x)$ becomes larger than Mg. It is seen in the figure that when the wheel reaches the position $x = 0.82L$, the wheel–beam contact force has its maximum, which is almost 2.5 times the static load Mg. This causes the wheel to continue moving upwards, and, as can be seen in the figure, the wheel will lose contact with the beam just before it reaches the support to the right.

This is the overall behaviour of the beam–mass system when the beam vibrates in its fundamental vibration mode. The more high-frequency variations of the contact force in Figure 6.10 are due to beam vibrations at higher modes. It should also be mentioned here that the speed v used is such that the time it takes for the wheel to pass the beam is half the eigenperiod of the beam at its fundamental frequency. The beam thus makes half a cycle in its fundamental mode during the time it takes for the wheel to pass the bridge. For an ordinary bridge, this normally gives a very high speed.

From this discussion it is concluded that in this case, with this mass ratio and speed, the "dynamic impact factor" is as large as 2.5, implying that due to dynamic effects the maximum mass-beam contact force is 2.5 times the static load. The dynamic impact factor depends on the mass ratio M/mL and vehicle speed v/v_{ref}, so other values than those used here will, of course, give other dynamic impact factors.

3. Beam (Rail) on Discrete Supports

To include also the pinned–pinned frequency in the track model, the continuous rail should be supported at discrete points. The supports could then be either discrete spring–damper systems or spring–mass–spring systems, modelling railpads, sleepers and ballast bed. One commonly used method to model this is to place the rail (a beam) on a spring and a damper in parallel. This spring–damper system models the railpad, below which is placed a rigid mass modelling the sleeper.

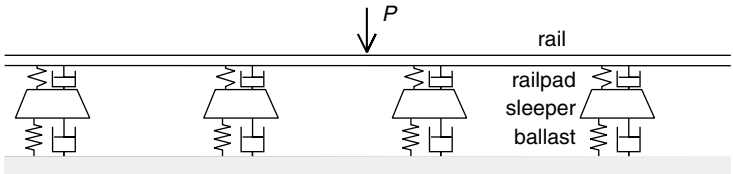

FIGURE 6.11 Rail on discrete supports. Rail is modelled as a beam (Euler–Bernoulli or Rayleigh–Timoshenko beam theory), the railpads are modelled by spring–damper systems, the sleepers are rigid masses, and the ballast is modelled by spring–damper systems.

The sleeper rests on an elastic foundation, i.e., another spring–damper system, see Figure 6.11. Using this track model, the three resonance frequencies described in Figure 6.3 can be captured, namely the track structure bouncing on the ballast, the rail and sleeper vibration with the railpad as a spring between the two masses, and the pinned–pinned frequency.

Sometimes, the rigid sleeper mass is replaced by a beam on an elastic foundation. The beam then extends perpendicularly to the rail, and the track model becomes three-dimensional. The sleeper in an elastic embedment is further discussed in Section IV.D.

4. Discretely Supported Track Including Ballast Mass

To be able to add a resonance frequency at low frequency (20 to 40 Hz) to the model described above, Oscarsson[41] incorporated more masses into the model, see Figure 6.12. By making the ballast and subgrade mass large (much larger than the sleeper and rail mass) and by adjusting the subgrade stiffness, a resonance at low frequency can be achieved. Then, essentially, the ballast-subgrade masses vibrate on the subgrade stiffness. It is noted in Figure 6.12 that there are connections between the ballast and subgrade masses, implying that a deflection at one point (at one sleeper) will influence the deflection at the adjacent sleepers. This phenomenon (which exists in a real track) cannot be modelled with the simpler models such as the track model in Figure 6.11. Zhai and Cai[42] used a similar model to investigate (among other things) the influence of the ballast density on the wheel–rail contact force at a rail joint and the ballast acceleration.

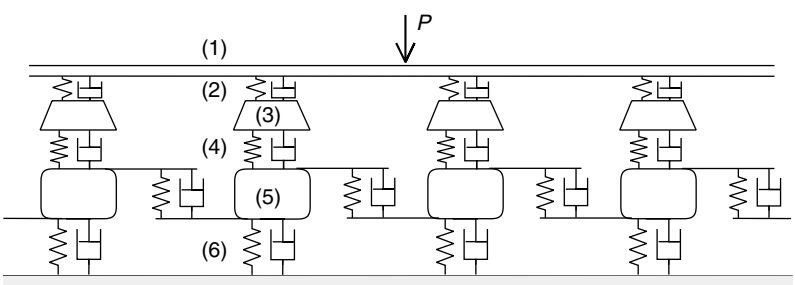

FIGURE 6.12 Rail on discrete supports with rigid masses modelling the sleepers. (1) Rail, (2) railpad stiffness and damping, (3) rigid sleepers, (4) ballast stiffness and damping. Rigid masses (5) below the sleepers represent the mass of the ballast and the subgrade, (6) subgrade stiffness and damping. By this model, the four resonance vibration modes (a) embankment vibration, (b) track-on-the-ballast vibration, (c) rail-on-railpad vibration, and (d) pinned–pinned vibration of the rail, may be captured (for (b), (c) and (d), see Figure 6.3).

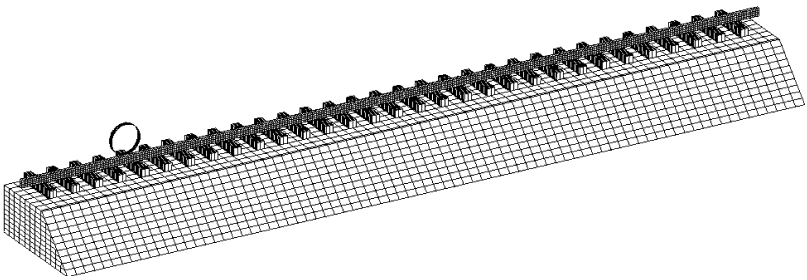

FIGURE 6.13 Rail on sleepers and the sleepers are embedded in a continuous ballast and subgrade medium. For the ballast and subgrade, three-dimensional finite elements are required. Symmetry with respect to the track centre-line is used here, implying that only half of the track needs to be modelled.

5. Rails on Sleepers Embedded in Continuum. Three-Dimensional Finite Element Models

The most realistic track model, and the model that normally requires the most computer capacity, is the model where rails and sleepers are modelled as beams (or possibly as three-dimensional bodies) with elastic elements modelling the railpads between the rails and the sleepers. The sleepers are embedded in a continuous medium. This requires that the track bed is modelled by three-dimensional finite elements. Figure 6.13 shows such a track model. Using a model like this, and also modelling a larger part of the surroundings, wave propagation from the track to the surroundings can be simulated. In the small model in Figure 6.13, nonreflecting boundary conditions must be used to avoid wave reflections at the boundaries.

H. Modelling of Dynamic Train–Track Interaction and Computer Program Developments

The dynamics of the compound train and track system plays an important role when investigating vehicle and track dynamics, ground-borne vibrations, and noise from the train traffic. Low-frequency (less than 20 Hz) motion of the train is crucial for assessment of safety and riding quality. High-frequency vibrations cause discomfort to passengers and emit noise and vibration to the surroundings. Also, vibrations may lead to track deterioration, such as railhead corrugation growth, damage to track components (railpads, fastenings, sleepers, ballast), track settlement, and so on.

In the early 1900s, Timoshenko published papers on the strength of rails, and later Inglis was active in this field. Early studies of the train–track interaction problem have been reviewed in the book by Fryba[43] (1972, 3rd ed. 1999). This book contains investigations on the vibrations of solids and structures under moving loads; the train (or wheel) then being modelled as a moving force. Knothe and Grassie[44] and Popp et al.[45] have presented state-of-the-art reviews in the field of train–track interaction.

Techniques to study the train–track interaction can be divided into two groups: frequency-domain techniques and time-domain techniques. These two techniques will be discussed in Section III.H.1 and Section III.H.2, respectively, and in Section III.H.3 examples of institutions developing computer programs for calculation of train–track interaction will be given.

1. Frequency-Domain Techniques

In the frequency-domain technique, receptances of the track are required (cf. Figure 6.3). If a stationary (not moving) wheel is loading the track, then the track receptance is needed only at

the point where the wheel is situated. The receptance (vertical or lateral, depending on what is studied) may be measured *in situ* on the track or it can be calculated using a track model. If a harmonically varying stationary load excites the track, then the direct receptance provides the track response.

Using the frequency-domain technique, it is possible to investigate the track and wheel response to a "moving irregularity." Instead of having a wheel moving on an uneven rail, one investigates a stationary wheel. The rail and the (stationary) wheel are then excited at the wheel–rail contact patch by a prescribed displacement. One may think of this excitation as if a strip of irregular thickness were inserted between the wheel and the rail. The strip is then forced to move between the wheel and the rail so that the irregularity of the strip will excite both wheel and rail. The response of the wheel and the track is obtained in the frequency domain. If the strip thickness irregularity is sinusoidal, the response is found from a receptance function. A nonsinusoidal irregularity (as from a wheel-flat) must first be transformed into the frequency domain by the Fourier transform. The track and wheel receptances and the wheel–rail contact stiffness are combined to form the appropriate transfer function. Together with the Fourier transform of the irregularity, the Fourier transform of the response is obtained, and the inverse transform provides the time-domain response. Several authors have used this technique to investigate the development of short wavelength corrugation on the railhead, see Section III.D.

If continuously supported rail is excited by a harmonically varying moving load, then the track response can be determined in a coordinate system following the load. The response is then assumed to be stationary. This topic has been thoroughly investigated in the book mentioned above, Fryba.[43] One method to treat a discretely supported rail is to develop the support reactions into Fourier series (making the support continuous but nonuniform) and then the moving load problem is solved with respect to a coordinate system following the load.

In the frequency-domain technique, only fully linear systems can be treated. The track responses are also assumed to be stationary, implying that singular events along the track, such as a rail joint, a sleeper hanging in the rail (not supported by the ballast), varying track stiffness, and so on, cannot be treated.

2. Time-Domain Techniques

When train–track dynamics are investigated in the time domain, deflections of the track and displacements of the vehicle are calculated by numerical time integration as the vehicle moves along the track. The vertical motion of the wheelset should then coincide with the vertical deflection of the rail, while taking the wheel–rail contact deformation into account. The wheel–rail contact force is unknown and has to be determined in the calculations.

The track can be modelled by finite elements, and in many cases a modal analysis of the track is performed. This requires that the track is modelled over a finite length. The track is then described through its modal parameters, and the physical deflections of the track are determined by modal superposition (this requires a linear track model). Often the vehicle is modelled by use of rigid masses, springs (linear or nonlinear) and viscous dampers. If a more detailed response of the vehicle is of interest, then a better vehicle model should be used and it could be convenient to also use modal analysis for the vehicle deformations (the vehicle is no longer composed of rigid bodies). Modal analysis of a wheelset makes it possible to include elastic deformations of the wheelset without a large increase of the number of degrees of freedom of the compound train–track system, Ripke[46] and Andersson.[47]

The modal analysis technique requires linear models. A finite element track model may also comprise nonlinear track elements. In such a model, the material properties may be selected to display the physical behaviour of the nonlinear track elements. Normally, nonlinearities can be found in railpads and in the ballast-subgrade material, see Oscarsson.[41] Nonlinearities in the track

have been treated as extra loads giving a force–displacement relationship for the track comparable with the nonlinear characteristics of the real track, Oscarsson.[41]

3. Computer Program Developments

A benchmark test of different train–track interaction models has been carried out, Grassie.[48] Both frequency-domain and time-domain models contributed to the test. In the test, eight sets of calculations were contributed, of which one was essentially from a low-frequency model, two contributions were from finite element models with calculations undertaken in the time domain, two were from finite element models with calculations undertaken in the frequency domain, and the remaining three were essentially analytical models with calculations undertaken in the frequency domain. In the time domain models and in two of the frequency domain models it was assumed that the rail was supported at discrete sleepers, while in the other frequency domain models a continuous support was assumed. The organisations or individuals who submitted results were:

- Dr S Grassie (private, program TRACK), U.K.
- Technical University, Berlin (two models), Germany
- Pandrol International Ltd, U.K.
- TNO (Nederlandse Organisatie voor Toegepast Natuurwetenschappelijk Onderzoek) in Delft (two models, program TWINS), The Netherlands
- Chalmers University of Technology, Gothenburg (program DIFF), Sweden, and
- University of Transportation and Communication, Zilina, Slovakia.

From the results of the benchmark test it was concluded that it was at least possible to obtain substantially similar results from both time domain and frequency domain models of vehicle–track interaction in the majority of circumstances considered in the test. Both types of models have attractions and disadvantages. It was concluded that the different types of model can be used with confidence in those areas where their attractions can be exploited in full. It can be mentioned here that the Swedish program DIFF has been further developed to comprise general three-dimensional motion of a train traversing the track, Andersson and Abrahamsson.[49]

Among other organisations developing train–track interaction models are:

- Spoornet, South Africa, see for example Fröhling,[50]
- Institute of Sound and Vibration Research, University of Southampton, U.K., see for example Wu and Thompson,[51]
- Technical University in Munich, Germany, see for example Dinkel,[52]
- Technical University in Milano, Italy, Diana et al.,[53]
- In the U.S.A., research is performed at the University of Massachusetts, Amherst, and at the Association of American Railroads, Transportation Technology at Pueblo, CO, Li and Selig[54]
- Train and Track Research Institute at Southwest Jiaotung University, Chengdu, P R of China, see for example Zhai W and Cai Z[42]
- Central Queensland University in Australia, Sun and Dhanasekar[55]
- Railway Technical Research Institute in Japan, Sato et al.[56]
- Linköping University, Sweden (author of this chapter)

IV. DYNAMIC PROPERTIES OF TRACK COMPONENTS

The most important parts of a track structure, from a track dynamics point of view, are the rails, sleepers or ties, railpads, fastenings, ballast, and the subgrade. Depending on what is to be studied,

these components may be modelled in a simpler or a more advanced manner. In this section, some track components will be investigated. The role and dynamic behaviour of the four components rail, railpad, sleeper, and ballast-subgrade will be examined in some detail.

A. The Rail

Here, the mathematical modelling of bending vibration of a free rail (and only the rail) will be treated. Therefore, there is no support along the rail; the rail is supported only at the boundaries. For bending vibration of a rail in the vertical plane, frequencies up to 3000 Hz are discussed. Below this frequency, beam theories can be used and the rail cross section can be considered not to change too much. At higher frequencies, the web and the flanges (the foot) of the rail start to vibrate. This is treated in this handbook in the chapter on noise. For lateral vibration, cross-section deformation becomes significant above 1000 Hz.

B. Mathematical Modelling of Rails

The rail may be modelled either as an ordinary Euler–Bernoulli (E–B) beam or as a Rayleigh–Timoshenko (R–T) beam. In the E–B beam theory, only the bending of the rail is taken into account, and in case of vibrations, only the mass inertia in translation of the beam is included. The differential equation describing the beam deflection $w(x,t)$ reads

$$EI\frac{\partial^4 w(x,t)}{\partial x^4} + \rho A\frac{\partial^2 w(x,t)}{\partial t^2} = q(x,t) \tag{6.4}$$

where EI is the bending stiffness of the beam, ρ is density, A is cross-sectional area, giving $\rho A = m$, which is the mass of the beam per metre (kg/m), and $q(x,t)$ is the load on the beam (t is time). The beam is supported at the ends only, i.e., at $x = 0$ and $x = L$ (beam length L is assumed). Damping of the beam is not included in this model. For stationary vibrations of the undamped beam, the solution to (the homogeneous part of) this equation may be written in the form

$$w_{\text{hom}}(x,t) = X(x)T(t) = X(x)\sin\,\omega t \tag{6.5}$$

where $X(x)$ gives the form of the beam deflection when it vibrates (the vibration mode) and ω is the vibration angular frequency.

The R–T beam theory includes rotatory inertia and shear deformation of the beam. In this case, two differential equations are needed to describe the vibrations. The deflection $w(x,t)$ and the shear deformation $\psi(x,t)$ are unknown functions. The differential equation for the deflection $w(x,t)$ becomes

$$EI\frac{\partial^4 w(x,t)}{\partial x^4} + \rho A\frac{\partial^2 w(x,t)}{\partial t^2} - \rho I\left(1+\frac{E}{kG}\right)\frac{\partial^4 w(x,t)}{\partial x^2\partial t^2} + \frac{\rho^2 I}{kG}\frac{\partial^4 w(x,t)}{\partial t^4}$$
$$= q(x,t) + \frac{\rho I}{kGA}\frac{\partial^2 q}{\partial t^2} - \frac{EI}{kGA}\frac{\partial^2 q}{\partial x^2} \tag{6.6}$$

where EI, ρ, A, and $q(x,t)$ are the same as in the E–B case, G is the shear modulus, and k is the "shear factor." Also, this equation (like the E–B one) describes the behaviour of the beam between the supports at the beam ends. A similar equation is obtained for the shear deformation $\psi(x,t)$.

If the shear deformation of the beam is suppressed, i.e., if one gives k a very large value, then the two last terms on both sides tend to zero. Further, if the mass inertia in rotation of the beam cross section is eliminated (noting that $\rho I = \rho r^2 A = mr^2$, and let r tend to zero), then the third term also tends to zero and the E–B differential equation is obtained.

In a state-of-the-art paper by Knothe and Grassie,[44] the authors state that shear deformation of the rail can be neglected only for frequencies below 500 Hz. Dahlberg[57] showed that at this

TABLE 6.1
Eigenfrequencies of a UIC60 Rail of Length $l = 4.2$ m

	Calculated			
Measured	$k = 0.34$	$k = 0.38$	$k = 0.40$	**E–B**
64	64.8	64.9	64.9	65.8
174	173	173	174	181
327	324	326	327	356
515	506	512	514	588
728	711	723	728	878
959	932	951	959	1227
1201	1163	1190	1202	1633
1450	1400	1437	1453	2098
1702	1640	1688	1710	2620
1955	1881	1942	1969	3201
2206	2123	2197	2230	3840
2456	2365	2452	2492	4537
2697	2606	2707	2753	—
2933	2846	2961	3013	—

Measured eigenfrequencies (in Hz) and calculated for some different values of the Timoshenko shear factor k (in factor kG). Last column provides eigenfrequencies obtained by the Euler–Bernoulli (E–B) beam theory.

frequency (500 Hz), and for a UIC60 rail, the Euler–Bernoulli beam theory provides a vibration frequency that is 10 to 15% too high, see Table 6.1 above.

An investigation of the significance of the rotatory inertia and the shear deformation of the rail was performed by Dahlberg.[57] Eigenfrequencies of some pieces of rails were measured and also calculated by use of Euler–Bernoulli and Rayleigh–Timoshenko beam theory. Different values of Timoshenko's shear factor k (in kG) were tried and results were compared to the measured eigenfrequencies and to the frequencies calculated by the Euler–Bernoulli beam theory. Results are presented in Table 6.1 and in Figure 6.14.

From this investigation, it can be concluded that for a UIC60 rail (a rail with mass 60 kg per meter) the Euler–Bernoulli beam theory yields approximately 15% too high frequency at 500 Hz

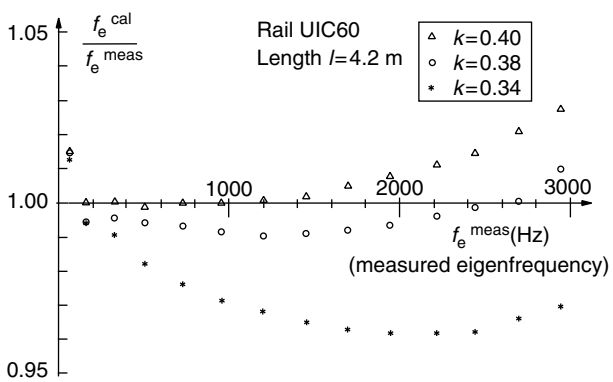

FIGURE 6.14 Influence of Timoshenko's shear factor k (in kG) for rail UIC60. Ratio of calculated eigenfrequency f_e^{cal} and measured eigenfrequency f_e^{meas} for rail of length $l = 4.2$ m.

and almost 30% too high frequency at 1000 Hz. For a 50 kg/m rail (the Swedish BV50 rail profile) the corresponding numbers are 12 and 30%, respectively.

In Figure 6.14, and also in Table 6.1, it can be seen that in order to obtain a good agreement between measured and calculated eigenfrequencies, the Timoshenko shear factor k should be different in different frequency intervals. The factor also depends on which rail is used. For the UIC60 rail and for frequencies below 1500 Hz, a reasonable value of k should be $k = 0.40$. For frequencies up to 3000 Hz, say, the k value could be somewhat lower ($k = 0.38$). For the BV50 rail, the value $k = 0.34$ gives a good fit over a large frequency range, see Dahlberg.[57] (It should be mentioned here that the widely used method to calculate the factor k proposed in Cowper[58] refers to static loading, and hence to static deflection, of the beam.)

Similar measurements and calculations of eigenfrequencies of concrete sleepers have been reported in Dahlberg and Nielsen,[59] see Section IV.D on sleeper vibration.

C. Railpads and Fastenings

In a track, the rails are fastened onto the sleepers. Usually, railpads are inserted between the sleepers and the rails, see Figure 6.2. The railpads provide electrical insulation of the rails and they protect the sleepers from wear. The railpads also affect the dynamic behaviour of the track. Grassie et al.[60] compared different track models with measurements and showed that it is important to include the railpads to obtain an accurate track model. Grassie and Cox[37] pointed out the importance of railpads when calculating the strains in the sleepers. The influence of soft and stiff railpads on the wheel–rail contact force and the track dynamics has been measured in full-scale experiments with a moving train, as reported by Fermér and Nielsen.[35] In those measurements, the train was equipped with an instrumented wheelset (with and without wheel flats) and the track was also equipped with measurement devices (strain gauges and accelerometers). Soft railpads were found to result in a lower sleeper acceleration and a higher railhead acceleration than the stiff railpads.

Laboratory measurements of stiffness and damping of studded rubber railpads have been performed by Thompson et al.[61] Also, Fenander[62] reported these measurements and compared them with field measurements on railpads. The stiffness of the railpads was found to be weakly dependent on frequency, but to increase strongly with preload. The damping loss factor of the railpads was found to be nearly independent of the preload and to increase only slightly with frequency.

The most commonly used physical model of a railpad is the spring–damper system, see Figure 6.11. The spring is usually assumed to be linear, and the damping is assumed to be proportional to the deformation rate of the railpad. It should be pointed out, however, that this viscous damping model does not always agree well with measured data (what may give a good fit at one train speed need not give a good fit at another speed). In practice, the damping is more or less independent of frequency, implying that a constant loss factor model agrees better.

As the stiffness of railpads has been found to increase strongly with preload (especially for studded railpads), a more accurate track model should display this behaviour, Wu and Thompson.[63]

Oscarsson[41] expanded a linear dynamic train–track interaction model to encompass nonlinear stiffnesses in the railpads and in the ballast. He undertook an investigation on the influence of the nonlinear railpad stiffness on rail corrugation growth (the growth of short wavelength periodic irregularities), and he found that a weak nonlinearity of the railpad stiffness does not influence the corrugation growth very much, whereas a strong nonlinearity may lead to an increased wear of the rail. Also, in Dahlberg,[64] a comparison of linear and nonlinear track models containing linear and nonlinear railpad stiffnesses was performed. It was shown that the axle load from the train distributes differently into the track in the linear and nonlinear track models.

A more advanced railpad model was set up by Fenander.[62] A fractional calculus model of the dynamic behaviour of railpads was proposed. Earlier, it has been shown that molecular theories for viscoelastic polymers can be used to derive the fractional derivative model, and that fractional derivative models accurately describe many viscoelastic materials by use of only few parameters.

This was exploited by Fenander, who used a four-parameter model to fit the measured stiffness and loss factor of the railpad. The fractional derivative model is linear. Therefore, for each preload level a new set of parameters had to be determined.

The role of the fastenings is normally neglected when investigating track dynamics. The fastenings should keep the rails in place (attached to the sleepers) and prevent the rail from rolling over when lateral forces are applied to it. The stiffness of the fastening is normally much less than that of the railpad. Therefore, when a wheelset loads the track, only the railpad stiffness is important. For an unloaded rail, however, the fastening will induce a certain preload (static load) on the railpad, and, knowing that the railpad stiffness is nonlinear, this may influence the dynamics of the unloaded track. The dynamic behaviour of rail fasteners at high frequencies has been investigated by Thompson and Verheij.[65]

D. The Sleepers

Railway track models sometimes contain beams (sleepers) on an elastic foundation. In this section the dynamic behaviour of free–free and *in situ* concrete sleepers will be treated. Two problems are faced: how to model the sleeper vibrations and how the elastic foundation supporting the *in situ* sleeper will influence the dynamic behaviour of it.

1. Sleeper Vibrations

Dynamic investigations of concrete sleepers are often made on sleepers with free–free boundary conditions, i.e., the sleeper is suspended in very soft springs, not influencing the vibration of the sleeper, so that the sleeper can be considered totally free. The free–free boundary conditions thus means that the two sleeper ends are free, see Figure 6.15. If Euler–Bernoulli beam theory is used to describe the sleeper vibration, good agreement between measured and calculated eigenfrequencies and eigenmodes is normally obtained only for the lowest two or three eigenfrequencies. To obtain a better agreement at higher frequencies, the more advanced Rayleigh–Timoshenko beam theory is required for the sleeper vibration calculations, Grassie.[66]

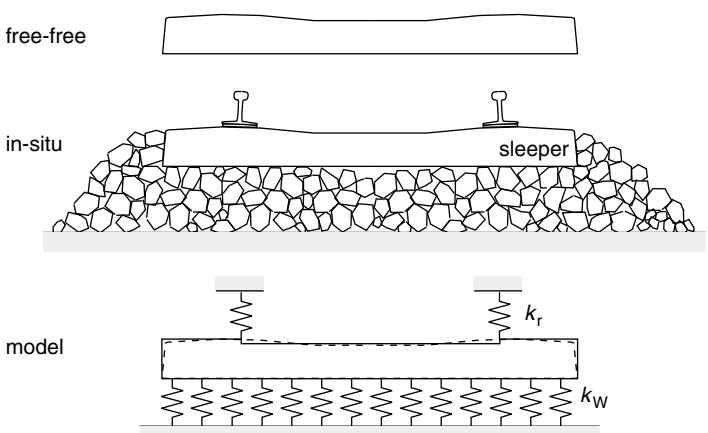

FIGURE 6.15 Free–free sleeper (top figure), *in situ* sleeper (sleeper in track), and model of the *in situ* sleeper. In the sleeper model, three beam elements were used. The sleeper is connected (via the rail) to the surrounding structure and is supported by distributed springs along the sleeper.

2. Elastic Foundation

The elastic bed of a sleeper in the track will influence the sleeper vibration. Therefore, eigenfrequencies of a beam on an elastic foundation will also be discussed. The eigenfrequencies (measured and calculated) of a free–free sleeper are compared with the frequencies of the same sleeper when it is placed in the track on the elastic foundation.

3. Measurements and Calculations

Measurements performed on free–free precast concrete railway sleepers give eigenfrequencies of the sleepers. Measured eigenfrequencies will be compared here with calculated frequencies obtained with the Euler–Bernoulli beam theory and with the Rayleigh–Timoshenko theory. The investigation summarised here was first reported in Dahlberg and Nielsen.[59]

Figure 6.15 shows the free–free sleeper, the sleeper in track, and the modelling of the sleeper. The physical, nonuniform sleeper used in the measurements was modelled as three uniform beams. The *in situ* sleeper rests on an elastic foundation (the ballast bed) and is connected to the surrounding structure via the rails. In the sleeper model, the elastic foundation is modelled by distributed springs along the sleeper, with spring stiffness k_W (N/m^2, i.e., spring stiffness N/m per metre of the sleeper). The connection of the sleeper to the rails and to other parts of the track (via the rail) is modelled by discrete springs, stiffness k_r (N/m), see Figure 6.15. For the central part of the sleeper, length 1.5 m, and for the two end parts, length 0.5 m each, beam elements were used with the following properties: bending stiffness $EI = 4.60$ and 6.41 MNm^2, mass $m = 91.2$ and 114 kg/m (giving a total sleeper mass of 251 kg), shear factor $kGA = 502$ and 628 MN, and radius of gyration $r = 0.0568$ and 0.0600 m, respectively (kGA and r are used in the R–T beam theory). Two different track beds were used, namely a soft bed, called *In situ* 1, with bed stiffness $k_W = 13$ MN/m^2 and "rail spring" stiffness $k_r = 17$ MN/m. For the stiffer bed, *In situ* 2, bed stiffness $k_W = 26$ MN/m^2 and "rail spring" stiffness $k_r = 34$ MN/m were used. Measured and calculated results are presented in Table 6.2.

The eigenfrequencies of a beam on an elastic foundation (i.e., the *in situ* sleeper) will differ from those obtained for the same beam if the beam is totally free. As can be seen in Table 6.2, the foundation induces two new eigenfrequencies (close to 80 Hz for the soft track and a little more that 110 Hz for the stiff track). These frequencies are marked 0 for the free–free sleeper and are two rigid-body motions of the free–free sleeper (rigid-body motion in translation and rotation).

TABLE 6.2
Eigenfrequencies of a Concrete Sleeper

Measured	Calculated			
free–free (Hz)	free–free E–B	free–free R–T	*In situ* 1 (soft)	*In situ* 2 (stiff)
0	0	0	79 (rotation)	111 (rotation)
0	0	0	82 (translation)	115 (translation)
113	121	118	131	143
335	347	327	335	344
639	696	624	631	637
995	1167	986	989	993
1390	1752	1391	1393	1394

Measured eigenfrequencies for free–free sleeper (in Hz) and calculated (also for free–free sleeper), using Euler–Bernoulli (E–B) and Rayleigh–Timoshenko (R–T) beam theory. Columns four and five (*in situ* sleeper) give eigenfrequencies of the same sleeper when it is placed in track, see Figure 6.15. Two different bed stiffnesses and rail stiffnesses were used (soft and stiff). The *in situ* frequencies have been calculated by use of the R–T theory.

The rigid-body motions of the free–free sleeper become two almost rigid-body eigenmodes (translation and rotation) of the *in situ* sleeper. It is also seen in the table that the lower eigenfrequencies in bending are influenced by the foundation stiffness and the "rail spring" stiffness, whereas higher eigenfrequencies are almost unaffected by these stiffnesses.

In Table 6.2, the two rigid-body motions of the free–free sleeper (frequency 0) become almost rigid-body motions of the same sleeper placed in the ballast bed (the stiffer bed makes these frequencies higher, of course). It is seen that the lowest bending mode, measured frequency 113 Hz, is obtained (fairly closely) both from the E–B theory and the R–T theory. This frequency increases some 10 to 15 Hz when the sleeper is placed in the track. The second bending mode, measured frequency 335 Hz, is also obtained (fairly closely) by the two theories, but it is seen that the E–B theory gives a slightly too high value here. This frequency is affected only a small amount by the track bed. At the third resonance frequency, the E–B theory gives almost 10% too high a value whereas the R–T theory is close to the measured one. This frequency is not greatly affected by the track bed. For the fourth and fifth frequencies, the E–B theory gives too large values whereas the R–T theory gives values very close to the measured ones. These frequencies are (more or less) unaffected by the support.

Thus, depending on which frequency interval is of interest, the concrete sleeper can be modelled as either a rigid mass (at frequencies below 100 Hz) or as a flexible beam. For frequencies up to 300 or 400 Hz, the Euler–Bernoulli beam theory may suffice. At higher frequencies, the Rayleigh–Timoshenko beam theory should be used for an accurate description of the sleeper vibration.

E. Ballast, Subballast and Subgrade

Placed under and around the sleepers, the ballast layer has several important functions:

- It limits sleeper movement by resisting vertical, transverse, and longitudinal forces from the trains
- It distributes the load from the sleepers to protect the subgrade from high stresses, thereby limiting permanent settlement of the track
- It provides necessary resilience to absorb shock from dynamic loading
- It facilitates maintenance surfacing and lining operations
- It provides immediate water drainage from the track structure
- It helps alleviate frost problems and
- It retards the growth of vegetation and resists the effects of fouling from surface-deposited materials.

At present, the state-of-the-art of track design concerning the ballast and the subgrade is mostly empirical. The factors that control the performance of the ballast are poorly understood. To assess the reasons why a particular section of track requires maintenance, it is necessary to know:

1. The characteristics of the ballast and subgrade
2. The maintenance history
3. The environmental history, and
4. The traffic history

Usually, only the last three items can be estimated from records. Information on the characteristics of the ballast and subgrade of an existing track is, in most cases, nonexistent. To gain information on the present conditions of a site, field examination is all that is possible.

As mentioned, the factors that control the performance of the ballast are poorly understood. In Knothe,[67] the long-term behaviour of the railroad track, including the ballast behaviour and the damage mechanisms underlying the ballast settlement, is discussed. Knothe states that any generally accepted damage and settlement equations do not exist, and hardly any material equations for the ballast itself. Only different suggestions to describe the ballast settlement from a phenomenological point of view are available; the settlement then being a function of number of loading cycles and/or magnitude of the loading.

1. Track Settlement

Railway track will settle (change its position) as a result of permanent deformation in the ballast and underlying soil. After having been used some time, the track will not be so straight and so well levelled as it was when it was new. The settlement is caused by the repeated traffic loading and the severity of the settlement depends on the quality and the behaviour of the ballast, the subballast, and the subgrade.

Track settlement occurs in two major phases:

- Directly after tamping, when the track position has been adjusted to a straight level, the settlement is relatively fast until the gaps between the ballast particles have been reduced and the ballast is consolidated.
- The second phase of settlement is slower and there is a more or less linear relationship between settlement and time (or load).

The second phase of settlement is caused by several basic mechanisms of ballast and subgrade behaviour:

- Continued (after the first phase) volume reduction, i.e., densification of the ballast and subground, caused by particle rearrangement produced by repeated train loading.
- Subballast and/or subgrade penetration into ballast voids. This causes the ballast to sink into the subballast and subgrade and the track level will change accordingly.
- Volume reduction caused by particle breakdown from train loading or environmental factors; i.e., ballast particles may fracture (divide into two or more pieces) due to the loading.
- Volume reduction caused by abrasive wear. A particle may diminish in volume due to abrasive wear at points in contact with other particles, i.e., originally cornered stones become rounded; then occupying less space.
- Inelastic recovery on unloading. Due to micro-slip between ballast particles at loading, all deformations will not be fully recovered upon unloading the track. In this case, the permanent deformation is a function of both stress history and stress state.
- Movement of ballast and subgrade particles away from under the sleepers. This causes the sleepers to sink into the ballast and subgrade.
- Lateral, and possibly also longitudinal (in the rail direction), movement of sleepers causing the ballast beneath the sleepers to be "pushed away," and the sleepers will sink deeper into the ballast.

Here, the first four items concern densification of ballast and subgrade, whereas the three last-mentioned items concern inelastic behaviour of the ballast and subgrade materials.

Concerning the volume reduction or densification caused by particle rearrangement produced by repeated train loading, it could be mentioned that the train load may also have an opposite effect. Due to the elastic foundation, the train load will lift the track (rails and sleepers) in front of and

behind the loading point, thus reducing or eliminating the preload (the dead load) caused by the rails and sleepers on the ballast. At the same time, due to the dynamic high-frequency train–track interaction forces, waves will propagate from the wheel–rail contact patches, either through the ballast and subgrade or through the track structure, to the region with the unloaded ballast. These waves will normally propagate faster than the train, giving vibrations in the unloaded ballast. This, in turn, may cause a rearrangement of the ballast particles so that the density decreases. As a result, this may cause a lift, at least temporarily, of the track.

2. Research on Ballast

A review of research on railroad ballast used as track substructure has been presented by Peplow et al.[68] The ballast materials and their interactions are complex from a physical point of view. Hence, appropriate constitutive laws for the (short-term) response of the materials have been developed including resilient modulus and variable modulus approaches. The laws are verified with respect to laboratory tests.

A historical method for assessing track performance is the use of track modulus. Its value for static and dynamic loading for track structure–ballast interaction is reviewed and discussed in Peplow et al.[68] For static loading, a comprehensive review of one approach is given. This approach uses multi-layer linear elastic static theory to represent the ballast and the subgrade layers. A number of finite element models have been developed and compared, and stresses incurred within the ballast and subgrade for various configurations are discussed.

For modelling the dynamic interaction between the track structure and the ballast, a simple beam on elastic foundation model (the Winkler foundation) is used in many analyses. In a number of studies a discrete support model with a finite number of parameters describing the rail, railpads, sleepers, and ballast mass and stiffness is used, see for example, Oscarsson[41] and Zhai et al.[69] In the final part of the survey by Peplow et al., modelling of the dynamic interaction between the train and the track structures is reviewed. The review also presents some mathematical and numerical methods dealing with the static and dynamic interaction of the train–track system and the substructure.

In Jacobsson,[70] a literature review of research on railroad ballast is presented, with emphasis on constitutive and mathematical modelling of the behaviour of ballast in tests. Different loading conditions in the tests are compression-tension, triaxial, and shear. Different mathematical descriptions of the constitutive behaviour of the material are given. In particular, descriptions of the resilient material properties and the evolution of permanent deformations, as a function of stress state, stress history, and the degree of compaction, are summarised.

The effect of different vehicles on track deterioration (and consequent maintenance costs) has been examined by Iwnicki et al.[71] A number of track settlement models were investigated. It was noted, for example, that the ORE (Office de Recherches et d'Essais de l'Union Internationale des Chemins de Fer) deterioration model contains no track parameters at all but only loading parameters such as traffic volume, dynamic axle load, and speed. Such a model, containing no track parameters, would imply that two different tracks, one stiff and one soft, would undergo the same deterioration if they were subjected to the same loading. This can be questioned, of course, since in such a case the quality of the ballast and subgrade material would have no influence on the track deterioration.

In Suiker,[72] advanced models were developed in order to provide detailed insight into short-term and long-term mechanical processes in a railway track. One of the purposes of the work was to derive enhanced continuum models from the discrete microstructure of a granular material (the ballast). The long-term mechanical process concerns the evolution of track deterioration as a result of a large number of train axle passages. A model that simulates the plastic deformation behaviour of the track bed during each loading cycle (wheel passage) would be unattractive.

Instead, a model is employed that captures only the envelope of the maximum plastic deformations generated during the cyclic loading of the track.

In a research programme in Germany, aimed at a better understanding of the dynamic interaction of vehicle and track and the long-term behaviour of the components of the entire system, settlement and deterioration of the ballast and the subgrade were examined. Nonlinear behaviour of the ballast was investigated experimentally in laboratories and simulated by new material laws, and the coupling of the track model and the subgrade was defined using various models, see Popp and Schiehlen.[73]

3. Modelling Track Settlement

The mathematical modelling of railway track settlement caused by inelastic behaviour of ballast and subground will now be discussed. In many track models the track stiffness and the track mass are modelled by discrete elements. The mass of the track is modelled with rigid bodies and the track stiffness is modelled with springs, see Figure 6.11 and Figure 6.12. In the model that will be discussed here, it is also assumed that the track settlement can be "discretized". Thus, the settlement of the track is collected in a "settlement element" in the track model.

For the purpose of modelling track settlement, a track model with a "settlement element" has been created, Dahlberg.[74] The model contains one rail (symmetry with respect to the centre line of the track is assumed), sleepers, ballast stiffness (spring elements), ballast damping, and an element beneath the ballast stiffness to take care of the permanent deformations in the ballast. The permanent deformation element thus models the track settlement (like a spring models the track stiffness), see Figure 6.16. The rail is modelled by finite elements, the (half)sleepers are rigid masses, the ballast springs have stiffnesses that may be linear or nonlinear, and the ballast damping is linear (modelled by viscous dampers).

The element taking care of the track settlement is modelled as a solid block (three-dimentional finite elements used) made of a linear elastic-ideally plastic material. This means that if the loading is not too high (i.e., below a threshold value, here the yield limit of the material), no settlement will occur. If, on the other hand, the threshold value (the yield limit) is exceeded, then plastic deformation will occur in the solid block. (It should be noted that this simple model was created to explore if it was possible to use a computer software to simulate the dynamic train–track interaction problem and to consider the track settlement in the same model. In a practical situation, a better model for the track settlement should be used, of course.)

The loading of the track comes from the moving wheel, which is loaded by a constant force: the dead load of the car body. The wheel mass and half of the axle mass are included, implying that the inertia force from the unsprung mass, i.e., the wheel and the axle, is taken into account.

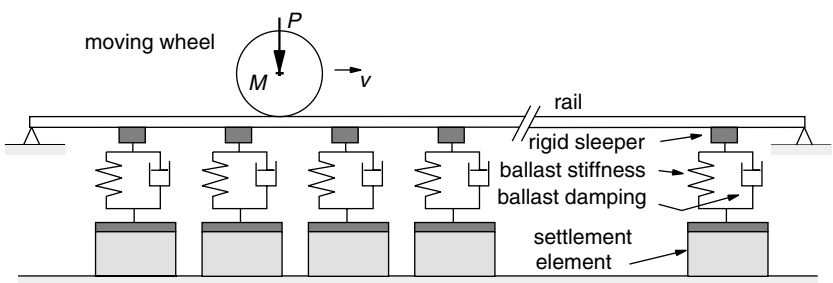

FIGURE 6.16 Model of railroad track containing rail, sleepers, ballast, and an element to model the track settlement. The model is loaded by the dead weight of the track structure (rail and sleepers) and by a moving mass (a wheel, mass M) subjected to a constant force P from the car body. Also, inertia forces of wheel and track are taken into account.

It was found that a large value of the yield limit of the settlement element material (all elements were elastic) would imply that the track returned to its original position after the wheel had passed (as expected, of course). A low value of the yield limit in some of the settlement elements resulted in a permanent deformation of the track after the wheel had passed. The level of the rail thus changed, giving a dip in the track at the place where the elastic–plastic settlement elements were placed.

V. SUMMARY

Dynamic properties of railway tracks have been surveyed. When a train moves on the track, the train, which is one dynamic system, interacts with the track, which is another dynamic system. Dynamic effects in the compound train–track system become more pronounced when train speed increases and when the axle load gets higher.

After the function of the track was introduced and dynamic properties of the track were discussed as a whole, several sources of dynamic excitation of the train and the track systems were discussed. Short wavelength irregularities on wheel and railhead induce high-frequency vibrations into the two systems (train and track), and so do impact loadings. Long wavelength irregularities, both in geometry and track stiffness, induce low-frequency oscillations and vibrations. The oscillations and vibrations then induce decreased ride comfort, increased track deterioration and noise emission.

Several mathematical models of the track structure were presented. These extended from the simple beam on Winkler foundation model to the more sophisticated three-dimensional finite element models, including rails, railpads, sleepers, ballast, and so on.

Modelling of the dynamic train–track interaction can be performed either in the frequency domain or in the time domain. Organisations and institutions developing computer programs dealing with the interaction problem were listed.

In the last part of this survey, dynamic properties of some track components (rail, railpad, sleeper, and ballast-subgrade), and mathematical modelling of them, were examined.

Finally, in addition to the textbooks and other books mentioned here, recent textbooks on railway engineering have been written by, for example, Esveld[75] and Profillidis.[76]

ACKNOWLEDGMENTS

Support by the following persons is gratefully acknowledged: calculations were performed by F. Månsson and A. Lundqvist at Linköping University. E. Berggren at Banverket (the Swedish National Rail Administration) provided Figure 6.6 (measurements performed by Banverket). Dr J. Nielsen at Chalmers University in Gothenburg has read the manuscript and commented upon it. Discussions with Prof David Thompson at the Institute of Sound and Vibration Research in Southampton, U.K., especially on the antiresonance effect in Figure 6.3, is gratefully acknowledged. This work was partly performed within the European FP5 programme GROWTH, project SUPERTRACK (Sustained Performance of Railway Tracks), contract No G1RD-CT-2002-00777.

REFERENCES

1. Li, D. and Selig, E. T., Evaluation of railway subgrade problems, *Transport. Res. Rec.*, 1489, 17–25, 1995.
2. Chrismer, S. and Read, D. M., Examining ballast and subgrade conditions, *Rail. Track and Struct.*, 90(6), 39–42, 1994.
3. Oscarsson, J., Dynamic train–track–ballast interaction: linear and state-dependent track models, *Thesis for the Dergee of Licentiate of Engineering*, Department of Solid Mechanics, Chalmers University of Technology, Gothenburg, Sweden, ISSN 0283-8672, 1999.

4. Jonsson, J., On ground and structural vibrations related to railway traffic, PhD thesis, Department of Structural Engineering, Chalmers University of Technology, Gothenburg, Sweden, 172 pp., 2000.
5. Krylov, V. V., Effects of the embankment topography and track curvature on ground vibration boom from high-speed trains, In *Proceedings of the Symposium EURODYN2002,* Munich, Germany, Grundmann and Schueller, Eds., Swetz & Zeitlinger, Lisse, pp. 473–478, ISBN 90 5809 510X, 2002.
6. Sato, Y., Matsumoto, A., and Knothe, K., Review on rail corrugation studies, *Wear*, 253(1–2), 130–139, 2002.
7. Alias, J., Characteristics of wave formation in rails, *Rail Int.*, 17(11), 17–23, 1986.
8. Lévy, D., Conception d'un système de mesure et d'analyse de l'usure ondulatoire des rails, *Revue Général des Chemins de Fer*, 108, 51–57, 1989.
9. Grassie, S. L. and Kalousek, J., Rail corrugation: characteristics, causes and treatments. Proceedings of the Institution of Mechanical Engineers, Part F, *J. of Rail and Rapid Transit*, 207(F1), pp. 57–68, 1993.
10. Kalousek, J. and Grassie, S., Rail corrugation: causes and cures, *Int. Rail. J.*, July, 24–26, 2000.
11. Clark, R. A., Dean, P. A., Elkins, J. A., and Newton, S. G., An investigation into the dynamic effects of railway vehicles running on corrugated rails, *J. Mech. Eng. Sci.*, 24(2), 65–76, 1982.
12. Igeland, A., Railhead corrugation growth explained by dynamic interaction between track and bogie wheelsets, Proceedings of the Institution of Mechanical Engineers, Part F, *J. of Rail and Rapid Transit*, 210(F1), pp. 11–20, 1996.
13. Clark, R. A. and Foster, P., On the mechanics of rail corrugation formation, *Proceedings of the Eighth IAVSD-Symposium the Dynamics of Vehicles on Roads and on Tracks*, held at the Massachusetts Institute of Technology, Cambridge, Massachusetts, August 14–19, 1983, Hedrick, J. K. Ed., Swets & Zeitlinger B V, Lisse, pp. 72–85, 1983.
14. Igeland, A., *Dynamic train–track interaction: simulation of railhead corrugation growth under a moving bogie using mathematical models combined with full-scale measurements*, PhD thesis, Division of Solid Mechanics, Chalmers University of Technology, Gothenburg, Sweden, 1997.
15. Werner, K., Diskrete Riffelabstände und die Suche nach den Ursachen der Schienenriffeln, *Zeitschrift für Eisenbahnwesen und Verkehrstechnik (ZEV) Glasers Annalen*, 110(10), 353–359, 1986.
16. Frederick, C. O., A rail corrugation theory, Contact Mechanics and Wear of Rail–Wheel Systems II, *Proceedings of the International Symposium*, Gladwell et al., Ed., University of Rhode Island, Kingston, R I, July 8–11, 1986, University of Waterloo Press, Waterloo, Ontario, Canada, pp. 181–211, 1987.
17. Brockley, C. A. and Ko, P. L., An investigation of rail corrugation using friction-induced vibration theory, *Wear*, 128, 99–106, 1988.
18. Valdivia, A. R., A linear dynamic wear model to explain the initiating mechanism of corrugation, *Proceedings of the Tenth IAVSD-Symposium the Dynamics of Vehicles on Roads and on Tracks*, held in Prague, August 24–28, 1987, Apetaur, M., Ed., Swets & Zeitlinger B V, Lisse, pp. 493–496, 1988.
19. Knothe, K. and Valdivia, A., Riffelbildung auf Eisenbahnschienen — Wechselspiel zwiscshen Kurzzeitdynamik und Langzeit-Verschleissverhalten, *Zeitschrift für Eisenbahnwesen und Verkehrstechnik (ZEV) Glasers Annalen*, 112(2), 50–57, 1988.
20. Knothe, K. and Ripke, B., The effects of the parameters of wheelset, track and running conditions on the growth rate of rail corrugations, *Proceedings of the 11th IAVSD-Symposium the Dynamics of Vehicles on Roads and on Tracks*, held in Kingston, Ontario, August 21-25, 1989, Anderson, R., Ed., Swets & Zeitlinger B V, Lisse, pp. 345–356, 1989.
21. Hempelmann, K. and Knothe, K., An extended linear model for the prediction of short-pitch corrugation, *Wear*, 191, 161–169, 1996.
22. Müller, S., *Linearized Wheel–Rail Dynamics — Stability and Corrugation*, Fortschritt-Berichte VDI, No 12-369, VDI-Verlag, Düsseldorf, 1998.
23. Suda, Y. and Iguchi, M., Basic study of corrugation mechanism on rolling contact in order to control rail surfaces, *Proceedings of the 11th IAVSD-Symposium the Dynamics of Vehicles on Roads and on Tracks*, held in Kingston, Ontario, August 21–25, 1989, Anderson, R., Ed., Swets & Zeitlinger B V, Lisse, pp. 345–356, 1989.
24. Kalousek, J., Keeping heavy haul track corrugation-free, *Rail. Gaz. Int.*, 145, 545–547, 1989.
25. Tassilly, E. and Vincent, N., A linear model for the corrugation of rails, *J. of Sound Vib.*, 150(1), 25–45, 1991.

26. Tassilly, E. and Vincent, N., Rail corrugations: analytical model and field tests, *Wear*, 144, 163–178, 1991.
27. Cervoni, G. and Vincent, N., Lutte contre l'usure ondulatoire des rails. Proposition d'une approche globale liant la voie et le matériel roulant, *Revue Général des Chemins de Fer*, 105(10), 559–570, 1986.
28. Bogacz, R., Brzozowski, M., Mahrenholtz, O., and Ronda, J., Dynamic effects in a rolling contact problem, *Zeitschrift für Angewandte Mathematik und Mechanik (ZAMM)*, 67(4), T176–T179, 1987.
29. Böhmer, A. and Klimpel, T., Plastic deformations of corrugated rails: a numerical approach using material data of rail steel, Proceedings of the Fifth International Conference on Contact Mechanics and Wear, Tokyo, Japan 2000, *Wear*, 253(1–2), pp. 150–161, 2001.
30. Nielsen, J. C. O., Numerical prediction of rail roughness growth on tangent railway track, *J. of Sound Vib.*, 267, 537–548, 2003.
31. Nielsen, J. C. O. and Johansson, A., Out-of round railway wheels — a literature survey, Proceedings of the Institution of Mechanical Engineers, Part F, *J. of Rail and Rapid Transit*, 214(F2), pp. 79–91, 2000.
32. Johansson, A., and Nielsen, J. C. O., Out-of-round railway wheels — Wheel–rail contact forces and track response derived from field tests and numerical simulations, Proceedings of the Institution of Mechanical Engineers, Part F, *J. of Rail and Rapid Transit*, 217(F2), pp. 135–145, 2003.
33. Andersson, C. and Dahlberg, T., Load impacts at railway turnout crossing, *Vehicle System Dynamics*, 33(Suppl.), 131–142, 1999.
34. Berggren, E., *Dynamic Track Stiffness Measurement– A New Tool for Condition Monitoring of Track Substructure*, Licentiate Thesis, Report TRITA AVE 2005:14, Railway Technology, Royal Institute of Technology (KTH), Stockholm, Sweden, 2005.
35. Fermér, M. and Nielsen, J. C. O., Wheel–rail contact forces for flexible versus solid wheels due to tread irregularities, Proceedings of the 13th IAVSD Symposium on Dynamics of Vehicles on Roads and on Tracks, Chengdu, Sichuan, China, August 23–27, 1993, *Vehicle Syst. Dyn.*, 23(suppl.), pp. 142–157, 1994.
36. Nielsen, J. C. O., *Train–track interaction, Coupling of moving and stationary systems — theoretical and experimental analysis of railway structures considering wheel and track imperfections*, PhD thesis, Division of Solid Mechanics, Chalmers University of Technology, Gothenburg, Sweden, 1993.
37. Grassie, S. L. and Cox, S. J., The dynamic response of railway track with flexible sleepers to high frequency vertical excitation, *Proc. of Inst. Mech. Eng., IMechE*, 198(D7), 117–123, 1984.
38. Månsson, F., *Simulation of dynamic train–track interaction considering track settlement*, MSc thesis, Department of Mechanical Engineering, Linköping University, Linköping, Sweden, Report LiTH-IKP-EX-1668, 2000.
39. Dahlberg, T., Vehicle–bridge interaction, *Vehicle Syst. Dyn.*, 13, 187–206, 1984.
40. Olsson, M., *Analysis of structures subjected to moving loads*, PhD thesis, Lund Institute of Technology, Division of Structural Mechanics, Report TVSM-1003, Lund, 1986.
41. Oscarsson, J., *Dynamic train–track interaction: linear and non-linear track models with property scatter*, PhD thesis, Department of Solid Mechanics, Chalmers University of Technology, Gothenburg, Sweden, ISSN 0346-718X, 2001.
42. Zhai, W. and Cai, Z., Dynamic interaction between a lumped mass vehicle and a discretely supported continuous rail track, *Comput. & Struct.*, 63(5), 987–997, 1997.
43. Fryba, L., *Vibration of Solids and Structures Under Moving Loads*, 3rd ed., Thomas Telford, London, ISBN 0-7277-2741-9, 1999.
44. Knothe, K. L. and Grassie, S. L., Modelling of railway track and vehicle–track interaction at high frequencies, *Vehicle Syst. Dyn.*, 22, 209–262, 1993.
45. Popp, K., Kruse, H., and Kaiser, I., Vehicle–track dynamics in the mid-frequency range, *Vehicle Syst. Dyn.*, 31(5–6), 423–464, 1999.
46. Ripke, B., Hochfrequente Gleismodellierung und Simulation der Fahrzeug-Gleis-Dynamik unter Verwendung einer nichtlinearen Kontaktdynamik, *Fortschritt-Berichte VDI*, Reihe 12 Nr 249, VDI-Verlag, Düsseldorf, 1995.
47. Andersson, C., *Modelling and simulation of train–track interaction including wear prediction*, PhD thesis, Department of Applied Mechanics, Chalmers University of Technology, Gothenburg, Sweden, 2003.

48. Grassie, S. L., Models of railway track and train–track interaction at high frequencies: Results of benchmark test, *Vehicle Syst. Dyn.*, 25(Suppl.), 243–262, 1996.
49. Andersson, C. and Abrahamsson, T., Simulation of interaction between a train in general motion and a track, *Vehicle Syst. Dyn.*, 38(6), 433–455, 2002.
50. Fröhling, R. D., *Deterioration of railway track due to dynamic vehicle loading and spacially varying track stiffness*, PhD thesis, Faculty of Engineering, University of Pretoria, Pretoria, South Africa, 1997.
51. Wu, T. X. and Thompson, D. J., Vibration analysis of railway track with multiple wheels on the rail, *J. Sound Vib.*, 239(1), 69–97, 2001.
52. Dinkel, J., *Ein semi-analytisches Modell zur dynamischen Berechnung des gekoppelten Systems Fahrzeug-Fahrweg-Untergrund für das Oberbausystem Feste Fahrbahn*, PhD thesis, Technische Universität, München, Germany, ISSN 0941-925X, 2001.
53. Diana, G., Cheli, F., Bruni, S., and Collina, A., Interaction between railroad superstructure and railway vehicles, *Vehicle Syst. Dyn.*, 23(Suppl.), 75–86, 1994.
54. Li, D. and Selig, E. T., Wheel/track dynamic interaction: track substructure perspective, *Vehicle Syst. Dyn.*, 24(Suppl.), 183–196, 1995.
55. Sun, Y. Q. and Dhanasekar, M., A dynamic model for the vertical interaction of the rail track and wagon system, *Int. J. of Solids Struct.*, 39, 1337–1359, 2002.
56. Sato, Y., Odaka, T., and Takai, H., Theoretical analyses on vibration of ballasted track, *Q. Rep. Rail. Tech. Res. Inst. (Jpn.)*, 29(1), 30–32, 1988.
57. Dahlberg, T., Vertical dynamic train–track interaction — verifying a theoretical model by full-scale experiments, *Vehicle Syst. Dyn.*, 24(Suppl.), 45–57, 1995.
58. Cowper, G. R., The shear coefficient in Timoshenko's beam theory, *Trans. ASME, J. of Appl. Mech.*, 33, 335–340, 1966.
59. Dahlberg, T. and Nielsen, J. C. O., Dynamic behaviour of free–free and in-situ concrete railway sleepers, *International Symposium on Precast Concrete Railway Sleepers*, Madrid, Spain, pp. 393–416, 1991.
60. Grassie, S. L., Gregory, R. W., Harrison, D., and Johnson, K. L., The dynamic response of railway track to high frequency vertical excitation, Proceedings of the Institution of Mechanical Engineers, Part C, *J. Mech. Eng. Sci.*, 24(2), pp. 77–90, 1982.
61. Thompson, D. J., van Vliet, W. J., and Verheij, J. W., Development of the indirect method for measuring the high frequency dynamic stiffness of resilient elements, *J. of Sound Vib.*, 213, 169–188, 1998.
62. Fenander, Å., *Modelling stiffness and damping by use of fractional calculus, with application to railpads*, PhD thesis, Division of Solid Mechanics, Chalmers University of Technology, Gothenburg, Sweden, 1997.
63. Wu, T. X. and Thompson, D. J., Effects of local preload on the foundation stiffness and vertical vibration of railway track, *J. of Sound Vib.*, 219(5), 881–904, 1999.
64. Dahlberg, T., Dynamic interaction between train and non-linear railway track model, *Proceedings of the Fourth International Conference on Structural Dynamics, EURODYN2002*, Munich, Germany, 2–5 September, 2002, Grundmann, and Schuëller, Ed., Swetz & Zeitlinger, Lisse, ISBN 90 5809 510X, 2002.
65. Thompson, D. J. and Verheij, J. W., The dynamic behaviour of rail fasteners at high frequencies, *Appl. Acoust.*, 52, 1–17, 1997.
66. Grassie, S. L., Dynamic modelling of concrete railway sleepers, *J. Sound Vib.*, 187, 799–813, 1995.
67. Knothe, K., Wechelwirkung zwischen Fahrzeug und Fahrweg, *Zeitschrift für Eisenbahnwesen und Verkehrstechnik*, 122(5), 173–180, 1998.
68. Peplow, A. T., Oscarsson, J., and Dahlberg, T., *Review of research on ballast as track substructure*, Report F189, Department of Solid Mechanics, Chalmers University of Technology, Gothenburg, Sweden, ISSN 0349-8107, 1996.
69. Zhai, W. M., Wang, K. Y., and Lin, J. H., Modelling and experiment of railway ballast vibrations, *J. Sound Vib.*, 270, 673–683, 2004.
70. Jacobsson, L., *Review of research on railway ballast behaviour — Experimental findings and constitutive models*, Report F208, Department of Solid Machanics, Chalmers University of Technology, Gothenburg, Sweden, ISSN 0349-8107, 1998.

71. Iwnicki, S., Grassie, S., and Kik, W., Track settlement prediction using computer simulation tools, *Vehicle Syst. Dyn.*, 33(Suppl.), 2–12, 2000.
72. Suiker, A. S. L., *The mechanical behaviour of ballasted railway tracks*, PhD thesis, Delft Technical University, Delft, The Netherlands. Delft University Press, ISBN 90-407-2307-9, 2002.
73. Popp, K. and Schiehlen, W., *System Dynamics and Long-Term Behaviour of Railway Vehicles, Track and Subgrade*, Springer, Berlin, 2003, ISBN 3-540-43892-0.
74. Dahlberg, T., Some railroad settlement models — a critical review, Proceedings of the Institution of Mechanical Engineers, Part F, *J. of Rail and Rapid Transit*, 215(F4), pp. 289–300, 2001.
75. Esveld, C., *Modern railway track*, MRT-Productions, Duisburg, Germany, 1989, ISBN 90-800324-1-7, (new edition 2001).
76. Profillidis, V. A., *Railway Engineering*, 2nd ed., Ashgate, Aldershot UK, 2000.